On the consistency of methane retrievals using TCCON and multiple spectroscopic databases.

Edward Malina[1], Ben Veihelmann[1], Matthias Buschmann[2], Nicholas M. Deutscher[3], Dietrich G. Feist[4,5,6], and Isamu Morino[7]

[1]Earth and Mission Science Division, ESA/ESTEC, Keplerlaan 1, Noordwijk, the Netherlands.
[2]Institute of Environmental Physics, University of Bremen, Bremen, Germany.
[3]School of Earth, Atmospheric, and Life Sciences, Faculty of Science, Medicine and Health, University of Wollongong NSW 2522 Australia.
[4]Lehrstuhl für Physik der Atmosphäre, Ludwig-Maximilians-Universität München, Munich, Germany.
[5]Deutsches Zentrum für Luft- und Raumfahrt, Institut für Physik der Atmosphäre, Oberpfaffenhofen, Germany.
[6]Max Planck Institute for Biogeochemistry, Jena, Germany.
[7]Satellite Remote Sensing Section and Satellite Observation Center, Center for Global Environmental Research, National Institute for Environmental Studies, Onogawa 15-2, Tsukuba, Japan.

Correspondence: Edward Malina (edward.malina.13@alumni.ucl.ac.uk)

Abstract. The next and current generation of methane retrieving satellite instruments are reliant on the Total Carbon Column Observing Network (TCCON) for validation. Understanding the biases inherent in TCCON and satellite methane retrievals is as important now as when TCCON started in 2004. In this study we highlight possible biases between different methane products by assessing the retrievals of the main methane isotopologue $^{12}CH_4$. Using the TCCON GGG2014 retrieval environment, retrievals are performed using five separate spectroscopic databases from four separate TCCON sites (namely, Ascension Island, Ny-Ålesund, Darwin and Tsukuba) over the course of a year. The spectroscopic databases include those native to TCCON GGG2014 and GGG2020; the HIgh-resolution TRANsmission molecular absorption database 2016 (HITRAN2016); the Gestion et Etude des Informations Spectroscopiques Atmosphériques 2020 (GEISA2020) database; and the ESA Scientific Exploitation of Operational Missions - Improved Atmospheric Spectroscopy (SEOM-IAS) database. We assess the biases in retrieving methane using the standard TCCON windows and the methane window used by the Sentinel 5-Precursor (S5P) TROPOspheric Ozone Monitoring Instrument (TROPOMI) for each of the different spectroscopic databases.

By assessing the retrieved $^{12}CH_4$ values from individual windows against the standard TCCON retrievals, we find bias values of between 0.05 to 2.5 times the retrieval noise limit. These values vary depending on the window and TCCON site, with Ascension Island showing the lowest biases (typically < 0.5) and Ny-Ålesund or Tsukuba showing the largest. For the spectroscopic databases, GEISA2020 shows the largest biases, often greater than 1.5 across the TCCON sites, and considered windows. The TROPOMI spectral window (4190-4340 cm^{-1}) shows the largest biases of all the spectral windows, typically >1, for all spectroscopic databases, suggesting further improvements in spectroscopic parameters are necessary. We further assess the sensitivity of these biases to locally changing atmospheric conditions such as solar zenith angle (SZA), water vapour and temperature. We find evidence of significant non-linear relationships between the variation of local conditions and the retrieval biases based on regression analysis. In general, each site/database/window combination indicating differing degrees

of sensitivity, with GEISA2020 often showing the most sensitivity for all TCCON sites. Ny-Ålesund and Tsukuba shows the most sensitivity to local conditions variations, while Ascension Island indicates limited sensitivity.

Finally, we investigate the biases associated with retrieving $^{13}CH_4$ from each TCCON site and spectroscopic database, through the calculation of the $\delta^{13}C$ value. With the aim of assessing the consistency of $^{13}CH_4$ across the databases. We find high levels of inconsistency, in some cases >1000% between databases, suggesting more work is required to refine the spectroscopic parameters of $^{13}CH_4$.

1 Introduction

Methane is widely acknowledged to have a significant impact on the global climate (IPCC, 2014), but the processes via which it enters and is removed from the atmosphere are still poorly understood, with bottom-up (scaled up in-situ measurements) estimations of the global methane budget not agreeing with top-down estimations (models) (Kirschke et al., 2013; Saunois et al., 2019). This disconnect is one of many reasons that has led to the development of multiple satellite missions, with the aim of improving the knowledge of the global methane budget. The remote sensing of methane is fundamentally dependent on inferring atmospheric concentrations from the absorption of light at wavelengths unique to methane, otherwise known as spectral lines. Methane, like all gases, is composed of a number of isotopologues, for example $^{12}CH_4$ and $^{13}CH_4$ forming the main constituents of methane. The position and intensity of the spectral lines of these isotopologues are stored in large databases known as spectroscopic databases (Gordon et al., 2017). These databases are a considerable source of error in the retrieval of atmospheric methane abundances, due to the uncertainty of the position and the magnitude of these spectral lines. The uncertainty is less with more abundant isotopologues (for example $^{12}CH_4$), however rarer isotopologues (e.g.$^{13}CH_4$) can have far more uncertainty. Differences in the various available spectroscopic databases could lead to significant differences between satellite estimates of methane (Galli et al., 2012; Scheepmaker et al., 2016). Understanding the spectroscopic differences of methane isotopologues is an important step towards reducing these uncertainties in future satellite measurements, and further refine the databases.

The launch of the Sentinel 5-Precursor (S5P) satellite, with the TROPOspheric Monitoring Instrument (TROPOMI) instrument (Veefkind et al., 2012), and the future Sentinel 5 (S5) mission with its Ultra-Violet Near infrared Shortwave infrared (UVNS) instrument (Ingmann et al., 2012), represent a significant advancement in space-based Greenhouse Gas (GHG) remote sensing, building on a decade of progress from the Greenhouse Gases Observing Satellite (GOSAT) (Yoshida et al., 2013). Unlike GOSAT, TROPOMI and UVNS exploit the $4190 - 4340$ cm^{-1} spectral range, which has not been explored in detail from previous space-based instruments for methane retrievals. The Scanning Imaging Absorption spectrometer for Atmospheric CartograpHY (SCIAMACHY) (Bovensmann et al., 1999) onboard the ENVIronmental SATellite (ENVISAT) was sensitive to this spectral range, but was plagued with detector issues (ice build-up). The Measurements Of Pollution In The Troposphere

(MOPITT) instrument (Drummond and Mand, 1996) is also sensitive to this spectral range, but is also affected by technical issues and has never successfully retrieved methane in this spectral window. The follow-on to GOSAT (GOSAT-2) also uses this spectral range; processing for GOSAT-2 is currently on-going. In addition, the wide spectral sensitivity of the limb viewing Canadian Atmospheric Chemistry Experiment (ACE)- Fourier Transform Spectrometer (FTS) (Bernath et al., 2005) includes this spectral window, but again the methane products of ACE-FTS do not include retrievals in this window. S5P/TROPOMI and S5/UVNS therefore rely on spectroscopic parameters for which only limited experience is available in their application to space-based methane retrieval instruments (Checa-Garcia et al., 2015; Galli et al., 2012). TCCON, although sensitive to this spectral range, has primarily provided its methane abundances retrieved from the 6000 cm^{-1} spectral region, allowing for direct comparisons with SCIAMACHY and GOSAT.

TCCON is a global network of 27 ground based Fourier Transform Spectrometers (FTS) (Wunch et al., 2010), with the primary aim of providing reference total column (a weighted average value for a nadir viewing profile) abundances of numerous atmospheric species calibrated against aircraft profiles (Wunch et al., 2010, 2011), including methane, for validation and cross-calibration purposes. TCCON operates in a wide spectral range (4000 – 11000 cm^{-1}) and records direct solar spectra. TCCON is currently one of the key sources of reference data for the validation of satellite-based GHG retrievals, e.g. the Orbiting Carbon Observatory (OCO)-2, GOSAT and TROPOMI (Yoshida et al., 2011; Crisp et al., 2012; Lorente et al., 2021). TCCON instruments have both high spectral resolution (0.02 cm^{-1}), and high Signal to Noise Ratios (SNR) due to direct solar viewing geometry, and insensitivity to atmospheric scattering, thus making TCCON measurements higher quality than satellite measurements and excellent comparison datasets for satellite retrievals. TROPOMI and UVNS both have overlapping spectral windows with the wide spectral range of TCCON within the Shortwave Infrared (SWIR) methane absorption regions, 5970-6289 cm^{-1} for UVNS and 4190-4340 cm^{-1} for UVNS and TROPOMI.

When validating methane products from TROPOMI and UVNS, retrieval products using the 4190 – 4340 cm^{-1} window will be compared with TCCON methane products generated using the standard TCCON windows 1) 5880-5996 cm^{-1}, 2) 5996.45-6007.55 cm^{-1} and 3) 6007-6145 cm^{-1}. Therefore potential biases associated with the choice of fit windows should be quantified and understood. Indeed, if the 4190 – 4340 cm^{-1} window proves to be as accurate as the standard TCCON windows, then there is justification to integrate TCCON retrievals from this window into future TCCON retrieval products. In addition, numerous algorithms will be used to provide methane data products from TROPOMI/UVNS (Hu et al., 2016; Schneising et al., 2019), which may use differing spectroscopic databases and are therefore subject to differing biases. Building on examples of similar past studies (Checa-Garcia et al., 2015; Galli et al., 2012), the high SNR and high spectral resolution makes TCCON data an excellent resource to assess any potential variations due to differences in the spectroscopic databases. By investigating the biases present in TCCON observations made at several sites over several seasons. We can infer some of the potential spectroscopic related biases in satellite retrievals, and their dependencies on local conditions such as water vapour that are relevant to ongoing TROPOMI validation, and future S5/UVNS validation. Note that the spectral resolution of TCCON is typically significantly higher than that of TROPOMI and other satellite instruments, which are unlikely to affected to the same degree as TCCON.

In addition to assessing the window and spectroscopic source biases for the main methane isotopologue $^{12}CH_4$, the opportunity is taken to retrieve the second most abundant isotopologue $^{13}CH_4$, and from this calculate the $\delta^{13}C$ value (see Eq 1). $\delta^{13}C$ requires the concentration of the two main methane isotopologues $^{12}CH_4$ and $^{13}CH_4$, which make up roughly 99% and 1% of global atmospheric methane respectively. Almost all measurements of this value are limited to in situ studies or airborne flask measurements, which although highly accurate, by their nature are spatially limited. Some effort has gone into satellite based retrievals of this metric (Buzan et al., 2016; Weidmann et al., 2017; Malina et al., 2018, 2019), but the results of these studies show this to be a challenging task. Therefore the calculation of the $\delta^{13}C$ value is a target of secondary importance in this study.

$$\delta^{13}C = \left(\frac{(^{13}CH_4/^{12}CH_4)_{sample}}{(^{13}CH_4/^{12}CH_4)_{VPDB}} - 1 \right) \times 1000\text{‰}, \tag{1}$$

where VPDB refers to Vienna Pee Dee Belemnite, an international reference standard for ^{13}C assessment. This is a quantity that has been used in numerous studies globally to differentiate methane source types (Fisher et al., 2017; Nisbet et al., 2016; Rigby et al., 2017; Rella et al., 2015), e.g. fossil fuel burning or wetlands. Tropospheric methane typically exhibits a $\delta^{13}C$ value of roughly -47‰ (Rigby et al., 2017), and total column measurements from TCCON should not deviate from this value to a significant degree. Therefore this tropospheric $\delta^{13}C$ value acts as a useful proxy, to determine the stability and variability associated with retrievals of methane isotopologues from different spectral windows, spectroscopic databases, location and time using the tropospheric $\delta^{13}C$ value as a baseline. In terms of $^{13}CH_4$, there are no published precision and accuracy requirements or statistics with TCCON. Calculating total column values of this metric would be highly beneficial for understanding the global methane budget, but is unlikely to be achievable with TCCON with an accuracy that would be sufficient for that purpose. However, calculation of $\delta^{13}C$ with TCCON will allow for an assessment of how far current technology is from making a useful total column assessment.

In this study, we use the TCCON GGG2014 (Toon, 2015) environment as the main tool for retrievals. Spectra are taken from four different TCCON sites in order to assess the impact of varying atmospheric conditions at different global locations. We assess the differences in abundances of the isotopologues and the quality of the fits when retrieved from standard TCCON spectral windows, and methane spectral windows in the TROPOMI/UVNS spectral range. We also quantify the variations in retrieval abundances when using five separate spectroscopic databases, and the application of non-Voigt line broadening shapes. Building on this assessment, the sensitivity of the retrievals to variations in water vapour concentration and path length are studied. This allows for the assessment of how differing windows and spectroscopic databases are sensitive to variations in local conditions.

This paper is structured as follows: section 2 outlines the methods used in this study, including details about the TCCON sites and spectra used, as well as the retrieval method. Information about the spectroscopic databases used in this study are also given. The results of this study are shown in section 3 outlining the biases between sites and databases, including an assessment of the sensitivity of the retrievals to local condition variability. Section 4 discusses the results shown in sections 3, and conclusions are drawn in section 5.

2 Methods, tools, datasets and requirements

2.1 TCCON sites used in study

We use TCCON spectra from four different sites identified in Table 1. Datasets over a single year were chosen in order to represent a wide range of seasonal conditions. The years chosen represent the years with maximum data coverage for each site respectively.

Table 1. TCCON sites used in this study.

TCCON Site	Lat/Lon	Date Range	Number of Spectra	Conditions
Ascension Island, Atlantic ocean	7.92°S, 14.3°E	Jan-Dec 2015	1518	Arid, little precipitation subject to some seasonal variation.
Darwin, Australia	12.5°S, 130.9°E	Jan-Dec 2020	39160	Tropical, significant water vapour background.
Ny-Ålesund, Spitsbergen	78.9°N, 11.9°E	April-Oct 2019	6315	Cold, dry, limited short-term variability.
Tsukuba, Japan	36.1°N, 140.1°E	Jan-Dec 2020	6162	Seasonal, cold dry winters, hot wet summers.

The TCCON sites used in this study were picked to have a wide range of conditions, with Ny-Ålesund capturing spectra in largely unvarying conditions with high SZA and low water vapour, while Ascension Island is similar in unvarying conditions although with higher background water vapour conditions and lower SZAs. This is contrasted by Darwin and Tsukuba which capture spectra under a wide range of SZAs and highly variable water vapour conditions. The mean background conditions for each site, as well as the variations over the dataset periods shown in Table 1 are indicated in Table 2. Significant variations in conditions and SZA are apparent between the TCCON sites, suggesting a wide range of capture conditions. We note the distributions of the conditions shown in Table 2 may not be normally distributed, but these statistics serve as a useful baseline to show the condition variations between the sites.

Table 2. TCCON sites water vapour, temperature and SZA average and variation.

TCCON Site	Water Vapour mean $\pm\sigma$	Temp mean $\pm\sigma$	SZA mean $\pm\sigma$
Ascension Island	4510 ppmv $\pm$ 890	27.5 $\degree\pm$ 1	38$\degree\pm$ 18
Darwin, Australia	5430 ppmv $\pm$ 1740	30.9$\degree\pm$ 3	45$\degree\pm$ 18
Ny-Ålesund, Spitsbergen	1440 ppmv $\pm$ 600	1.7$\degree\pm$ 6	69$\degree\pm$ 8
Tsukuba, Japan	3200 ppmv $\pm$ 2470	22.9$\degree\pm$ 9	50$\degree\pm$ 18

2.2 GFIT Retrieval Algorithm

In this study, we use the GGG2014 environment, which includes the GFIT retrieval algorithm (Wunch et al., 2010), summarised briefly here. GFIT employs a nonlinear least-squares fitting scheme: a forward model (radiative transfer model which simulates radiation transfer through an atmosphere or a body of gas) is used to calculate synthetic irradiance spectra based on a set of
135 parameters known as state vector elements (typically trace gas concentrations) and model parameters (e.g. temperature and pressure profiles). These synthetic irradiance spectra are then fitted to the measured irradiance spectra by adjusting the state vector elements to provide a final result, normally a trace gas abundance. In the case of GFIT, the state vector can include the following.

   – first target gas scaling factor (desired output).

140   – interfering gas scaling factor.

   – continuum level of the irradiance spectrum.

   – continuum tilt

   – continuum curvature

   – frequency shift

145   – zero level offset

   – solar scaling (differences in shifts of atmospheric and solar lines)

   – fit channel fringes

Note that not all of the above are routinely included in the state vector, especially the continuum curvature which is not commonly included in the state vector. This option is designed to remove instrument features, but may also attempt to remove
150 other effects due to the spectroscopic database, as noted in the TCCON wiki (TCCON, 2020). GFIT assumes a fixed profile

shape for each trace gas, and the sub-column amounts for each altitude/pressure level are not independently scaled. Unlike in most satellite retrieval algorithms, aerosol and albedo terms are not included in the state vector, because TCCON operates in direct solar viewing, where scattering is considered unimportant and surface terms are not necessary. The retrieved trace gas column is calculated by multiplying scaling factors from the retrieved state vector by the a priori vertical column abundances.

155 The TCCON a priori profiles are obtained from the National Centers for Environmental Prediction/National Center for Atmospheric Research analyses for temperature, pressure and humidity. Combined with empirical models for CO_2, CO, CH_4 and N_2O developed from FTS balloon flights, data from the ACE-FTS instrument (Wunch et al., 2011). Dry air Mole Fractions (DMF) are calculated by dividing the scaled trace gas column with the total column O_2, retrieved from a wide window in the 7885 cm^{-1} spectral region multiplied by the volume mixing ratio of O_2 0.2095. We use O_2 from GGG2014 only, to provide

160 a point of consistency between the spectroscopic databases, and because SEOM-IAS does not include spectral lines in this region. DMF gas volumes identify retrieved abundances as mole fractions, as opposed to absolute concentrations, all retrieved $^{12}CH_4$ abundances are referred to as DMF values.

Because of the high spectral resolution of the TCCON instruments (0.02 cm^{-1}), most spectral lines are resolved, therefore radiative transfer calculations are performed on a line-by-line basis. GGG includes a spectroscopic database in its environment, which is similar to other more widely adopted databases. TCCON has a standard set of spectral windows for methane retrievals,

165 all of which are in the 6000 cm^{-1} methane absorption window range. In this study we include the TROPOMI/UVNS SWIR spectral windows. This window, along with a description of all of the windows considered in this study are described in Table 3 below.

Table 3. Spectral windows used in study.

Window	Window spectral range (cm^{-1})	Target species	Background species	Window source
1	4190-4340	$^{12}CH_4$	CO_2, H_2O, HDO, CO, HF, N_2O, O_3	Sentinel 5 baseline
2	5880-5996	$^{12}CH_4$	CO_2, H_2O, N_2O	TCCON standard
3	5996.45-6007.55	$^{12}CH_4$	CO_2, H_2O, N_2O, HDO	TCCON standard
4	6007-6145	$^{12}CH_4$	CO_2, H_2O, N_2O, HDO	TCCON standard

Windows 2-4 are standard TCCON methane retrieval windows which in this study are used for $^{12}CH_4$, and window 1 is

170 based on the TROPOMI spectral window (Galli et al., 2012; Hu et al., 2016), given that no standard windows exist in this

spectral window for TCCON. In addition, TCCON methane products are the result of a standardised process where a weighted average of three retrieved values from windows 2, 3 and 4 described in Table 3 (Cal, 2022).

For $^{13}CH_4$ retrievals, windows 1 and 4 are used.

2.3 Spectroscopic Databases

175 We use parameters from five separate spectroscopic databases, which are as follows: 1) The database included with GGG2014 (Toon, 2015), which currently assumes a Voigt line shape for all lines. 2) The database included with the updated GGG2020 software, referred to in this study as GGG2020, which includes numerous updates to the GGG2014 spectroscopic parameters. Some non-Voigt parameters are included in GGG2020, but are not exploited in this study, because GGG2014 was not modified to take advantage of them. 3) HITRAN2016, which is a well-established spectroscopic database that has been used in 180 numerous satellite based studies previously (Galli et al., 2012). Methane has been updated in the current release HITRAN2016 (Gordon et al., 2017) from the previous release (HITRAN2012), with new lines and parameters included for both of the main isotopologues. HITRAN2016 includes the additional parameters required to model non-Voigt lines shapes, however the current version does not include these parameters for methane (at the time of writing). 4) The GEISA2020 database (Delahaye et al., 2021) is another spectroscopic database, similar in design and goals to the HITRAN databases. The GEISA database 185 does not currently include non-Voigt line shape parameters. 5) SEOM-IAS (Birk et al., 2017), specifically developed for the TROPOMI spectral window and designed around non-Voigt atmospheric line shape profiles. This database only has data within the 4190-4340 cm^{-1} spectral range, and can therefore only contribute to window 1 of this study.

For clarification purposes, there are no official releases of the spectroscopic parameters used in the GGG TCCON retrievals. We refer to the databases used in this study as GGG2014 and GGG2020 in order to differentiate with them, based on the GGG 190 retrieval environment releases, with GGG2020 due for release in the near future (Laughner et al., 2021).

Some work has been performed previously comparing spectroscopic databases e.g. (Jacquinet-Husson et al., 2016; Armante et al., 2016), generally indicating that the need to resolve differences between spectroscopic databases remains. Yet none have specifically targeted the TROPOMI SWIR spectral region, therefore this study is the first case with respect to the TROPOMI spectral window with TCCON.

195 Beyond exploring the impact of differing spectroscopic database parameters, we investigate the use of non-Voigt broadening parameters. Ngo et al. (2013) find the standard Voigt profiles used for spectral line broadening may be inadequate for trace gas retrievals (based on laboratory studies), which can lead to errors larger than instrument precision requirements. In order to calculate more accurate line shapes for remote sensing purposes, numerous models have been proposed. In this paper we use the quadratic Speed Dependent Hard Collision (qSDHC) model (Ngo et al., 2013; Tran et al., 2013). This model includes additional 200 parameters based on speed dependence of collisional broadening and velocity changes of molecules due to collisions, on top of the standard parameters of pressure-induced air broadening, and pressure induced line shift. Note that only the SEOM-IAS database uses these additional parameters, the remaining spectroscopic databases do not include these parameters for methane at the time of this paper. We use the FORTRAN routines provided with Ngo et al. (2013) to implement the qSDHC model into the GFIT algorithm, modified to include first order Rosenkranz line-mixing effects. Mendonca et al. (2017) report

205 that incorporating speed dependent and line-mixing has a significant effect on calculated methane columns when compared against assuming Voigt dependency. They find a +1.1% difference in total methane column abundances from 131,124 spectra. The implication is that it is important to account for the additional physical parameters included in non-Voigt models, when retrieving methane.

We note the introduction of $^{13}CH_4$ into spectroscopic databases in the TROPOMI spectral region is relatively recent, and in 210 the case of HITRAN, was only introduced in the 2012 release (Brown et al., 2013), thus suggesting that $^{13}CH_4$ spectroscopic parameters may retain high levels of uncertainty.

2.4 Analysis structure and metrics

The following section describes the assessment metrics used in this study. Firstly we assess the quality of the fit of the measured and modelled spectra for each window indicated in Table 3 for each spectroscopic database at each TCCON site. The quality 215 of the fit is expressed through Root Mean Square Error (RMSE) of the residual between the calculated transmission spectra, and the TCCON measurement transmission spectra, and the χ^2 test, quantitatively defined as:

$$\chi^2 = \sum_i [\mathbf{y_{measured}} - \mathbf{y_{calculated}}]^2. \tag{2}$$

.

Where $\mathbf{y_{measured}}$ refers to the measured TCCON spectrum, and $\mathbf{y_{calculated}}$ is the synthetic spectrum calculated by the 220 forward model. Secondly we assess the variance of the calculated DMFs of $^{12}CH_4$ for each window, spectroscopic database and TCCON site w.r.t the standard methane product used in TCCON retrievals currently, which is a weighted average of windows 2, 3 and 4. This variance is described through the RMSE in Eq. 3:

$$NRMSE = \sqrt{\sum^n \frac{\left(\frac{X^{12}CH_{4window} - X^{12}CH_{4standard}}{\sigma_{standard}}\right)^2}{n}}, \tag{3}$$

where NRMSE refers to the normalised RMSE, $X^{12}CH_{4window}$ is the retrieved DMF from a specific window, $X^{12}CH_{4standard}$ 225 is the retrieved DMF from the TCCON standard product, and $\sigma_{standard}$ is the retrieval error from the standard methane product. The variance is also given by the absolute mean residual described in Eq. 4:

$$NAmean = \left| \sum^n \frac{\left(\frac{X^{12}CH_{4window} - X^{12}CH_{4standard}}{\sigma_{standard}}\right)}{n} \right|, \tag{4}$$

where NAmean is the normalised absolute mean residual, and all other terms are as identified previously. Following the assessment of the retrieval variance between windows and databases, we investigate if locally changing conditions impact 230 biases between spectroscopic databases and windows. Variations in the retrieval conditions throughout the course of a day of measurements are included in TCCON error budgets, for example artefacts can appear in TCCON retrievals at extreme

SZA values (Wunch et al., 2011). We therefore investigate if the methane retrieval biases vary with respect to the following local parameters 1) SZA, where extreme angles can cause errors in the air-mass assumptions and affect characteristics of the Instrument Lineshape function (ILS) (Wunch et al., 2011); 2) Water vapour (retrieved by TCCON in two standard narrow windows) through the whole available data range at the respective TCCON sites. The GFIT retrieval algorithm is a scaling retrieval algorithm for all trace gas fitting, meaning that an incorrect a priori trace gas profile shape will yield errors in the retrieval. The GFIT water vapour a priori is based on a profile taken at midday for each specific retrieval, meaning that any significant variations from this daily profile will yield errors in the retrieval, that will vary depending on the impact of water vapour on a specific spectral window. 3) Temperature, which is not included in the retrieval state vector and dependencies on temperature will not be removed in the retrieval process. Temperature errors are introduced through the spectroscopic cross-sections (An et al., 2011), therefore poor knowledge of spectroscopic parameters will potentially lead to temperature based errors.

These dependencies are quantified by non-linear regression analysis, consisting of fitting the variations of water vapour, SZA and measured temperature against the normalised difference between each methane isotopologue DMF case and the DMFs from the standard TCCON methane retrieval window. Here the normalisation factor is the uncertainty from the standard TCCON methane retrieval.

The magnitude of the metrics defined above can be put into context by comparisons with the TCCON error budget. TCCON typically aims for precision of <0.3% on methane retrievals, and has a rough estimate of 1% systematic uncertainties (dominated by in-situ calibration which can affect sites differently (Wunch et al., 2015)). Therefore it is possible to judge the variation of $^{12}CH_4$ DMFs between windows and databases based on these biases and precision.

Finally, although the quality of the $^{13}CH_4$ fit metrics in this study are not covered in detail, we instead calculate $\delta^{13}C$ in order to understand the plausibility and variation of retrieving $^{13}CH_4$ from TCCON. Fundamentally the final aim of retrieving $^{13}CH_4$ is to calculate $\delta^{13}C$. How much $\delta^{13}C$ varies in the total column is a complex issue (Weidmann et al., 2017; Malina et al., 2018, 2019), in-situ studies (Nisbet et al., 2016; Rigby et al., 2017; Fisher et al., 2017) all show that an uncertainty of «1‰ in $\delta^{13}C$ is required in order to determine natural annual variability at the surface. However, variability in $\delta^{13}C$ can be higher in the troposphere and stratosphere due to variability of the OH sink and the fractionation caused by OH (Röckmann et al., 2011; Buzan et al., 2016), with evidence that $\delta^{13}C$ can vary by up to 10‰ in different air parcels (Röckmann et al., 2011). Based on these factors, we assume a rough total column $\delta^{13}C$ variability of 1‰, which equates to a total uncertainty of <0.02 ppb on $^{13}CH_4$ retrievals, or roughly 0.1% of the total column. This is clearly an unrealistic target for individual retrievals, given the uncertainty requirements for $^{12}CH_4$ described above. However, TCCON currently represents the best chance of remotely measuring $\delta^{13}C$, since precision errors are low and SNR is high (Wunch et al., 2011). In addition, because TCCON sites are situated in fixed positions long-term averaging is possible, which further reduces precision based errors. Therefore one of the minor aims of this study is to identify how far away TCCON uncertainty (including systematic errors) is from the desired uncertainty of <1‰ $\delta^{13}C$.

 # 3   Results

3.1   Quality of spectral fitting

An example of residual transmission spectra from the Ny-Ålesund site is shown in Fig 1, with the standard deviation of a selection of retrievals within the same time period indicated by the red lines. Examples of spectral fits from the other TCCON sites considered in the study are shown in the appendix. Qualitatively we note clear differences in the quality of the fits between

270   windows and databases, for example there are clear deviations apparent, especially in window 1 for HITRAN and GEISA.
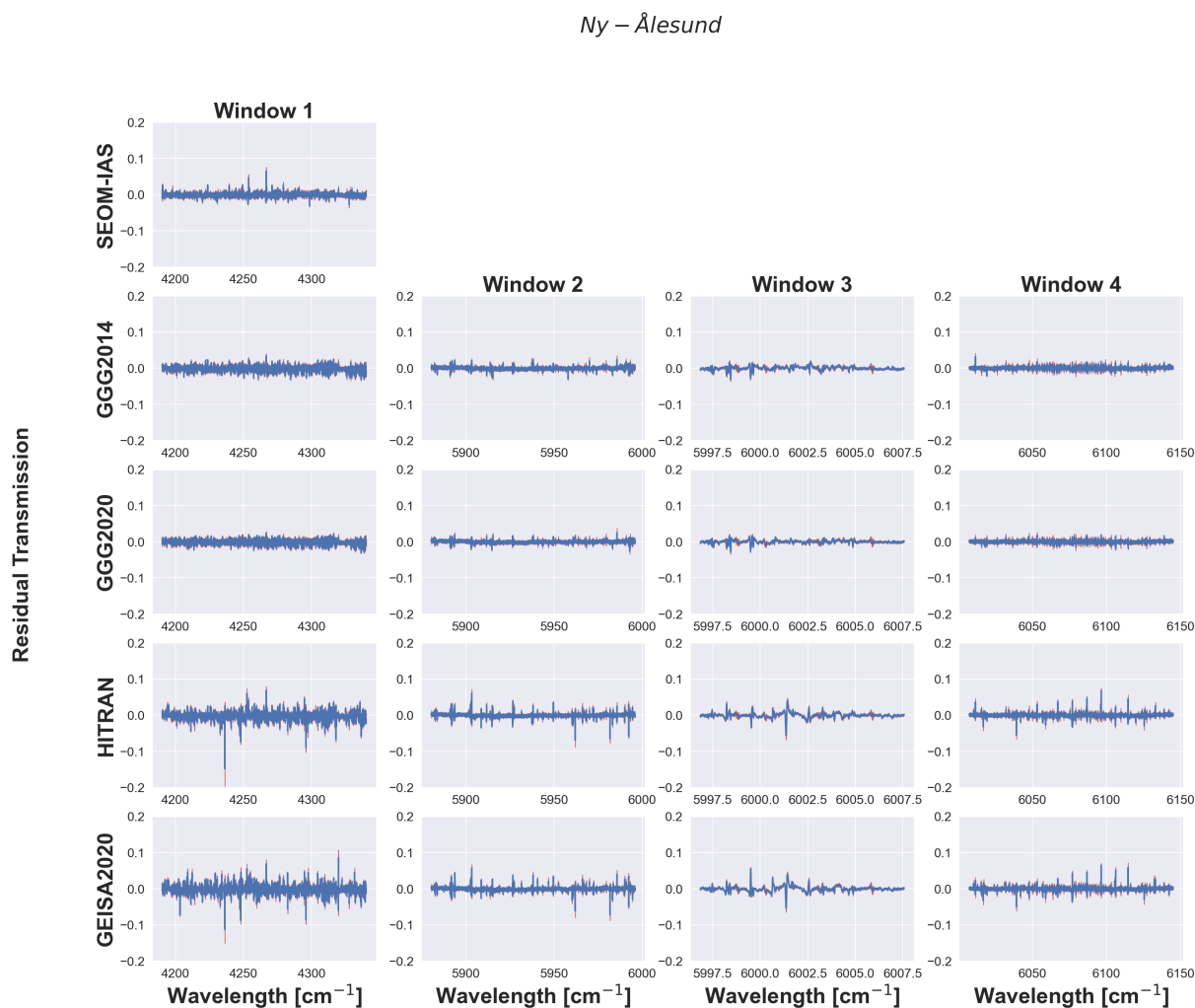
Figure 1. Example residual transmission spectra calculated from measured and fitted spectra from the Ny-Ålesund in 2019. The blue line indicates an example of the fit residual between the calculated transmission and the measured transmission. The red lines indicates the standard deviation of the residual, based on all spectra taken over the entire dataset. The columns of this figure identify the residuals of a specific window, and the rows a specific database, as identified in the axis labels.

The analysis statistics for the residual transmission spectra (as discussed in sect. 2.4) shown in Fig 1 are presented in Fig 2, as well as the associated statistics for the other TCCON sites considered in this study. What is clear from Fig 2 is that the fit statistics for each spectroscopic database, irrespective of TCCON site and window generally have the same pattern in terms of quality. For window 1 SEOM-IAS and GGG2020 are more or less equivalent in quality, followed by GGG2014, HITRAN and then GEISA. In windows 2-4 where SEOM-IAS has no data, GGG2020 typically shows the highest quality fits, suggesting the latest iteration of the GGG2020 spectroscopic parameters has superior performance to the older version.

Window 1 typically shows the poorest fit metrics of all windows, possibly because it is the largest window, but also because it is more complex region in terms of absorption (Brown et al., 2013) than the other windows. Window 4 for example is also wide, but typically shows higher quality fits than any of the other windows in this study. The implication being that the knowledge of spectroscopic parameters in window 1 is still lacking in comparison to the traditional TCCON windows.

There are differences in the metrics between TCCON sites, with Ascension Island showing poorer RMSE values than any of the other sites, similar to Darwin. This is to be expected however since these instruments are not identical, and capture spectra under differing conditions. We note that all instruments are run according to TCCON specifications but their respective configurations are not exactly the same. This is normal and necessary as different sites need local adjustments to account for different local conditions such as altitude, humidity or cloud conditions. Most of the effects caused by such individual configurations are removed by the differential CO_2 and CH_4 DMF retrievals but will affect individual spectra. For example, in the case of Tsukuba and Ascension, the configuration effects cannot be compared directly except for detector noise, which turned out to be comparable. However, the signal on the detector of the Ascension Island instrument is at least 50% lower than that of the Tsukuba instrument. Likely reasons for this difference are: 1) The Ascension FTS runs on a higher spectral resolution (0.014 cm^{-1} vs. 0.02 cm^{-1}) and a faster scanner speed (10 kHz vs. 7.5 kHz). Both reduce integration time per spectral pixel. 2) The illumination of the InGaAs detector on Ascension is kept low on purpose to avoid saturation. This setting cannot be readjusted in between site visits and has to last for months. Other sites may use similar techniques, and may vary depending upon need. 3) The solar tracker has known issues with pointing at the centre of the sun at low SZAs but cannot be replaced easily. In addition, dust buildup on the solar tracker mirrors reduces the reflectively of the mirrors quickly. They are cleaned weekly but a signal loss in the order of 20% over a few days is not uncommon.

The results from Tsukuba are different from the other showcased results, this is likely because of the smaller amount of spectra available for plotting (owing to data transfer and storage limits). There was no limit in the actual retrievals identified in the following paper sections.

Example transmission spectra for Darwin, Tsukuba and Ascension Island are identified in Appendix A.
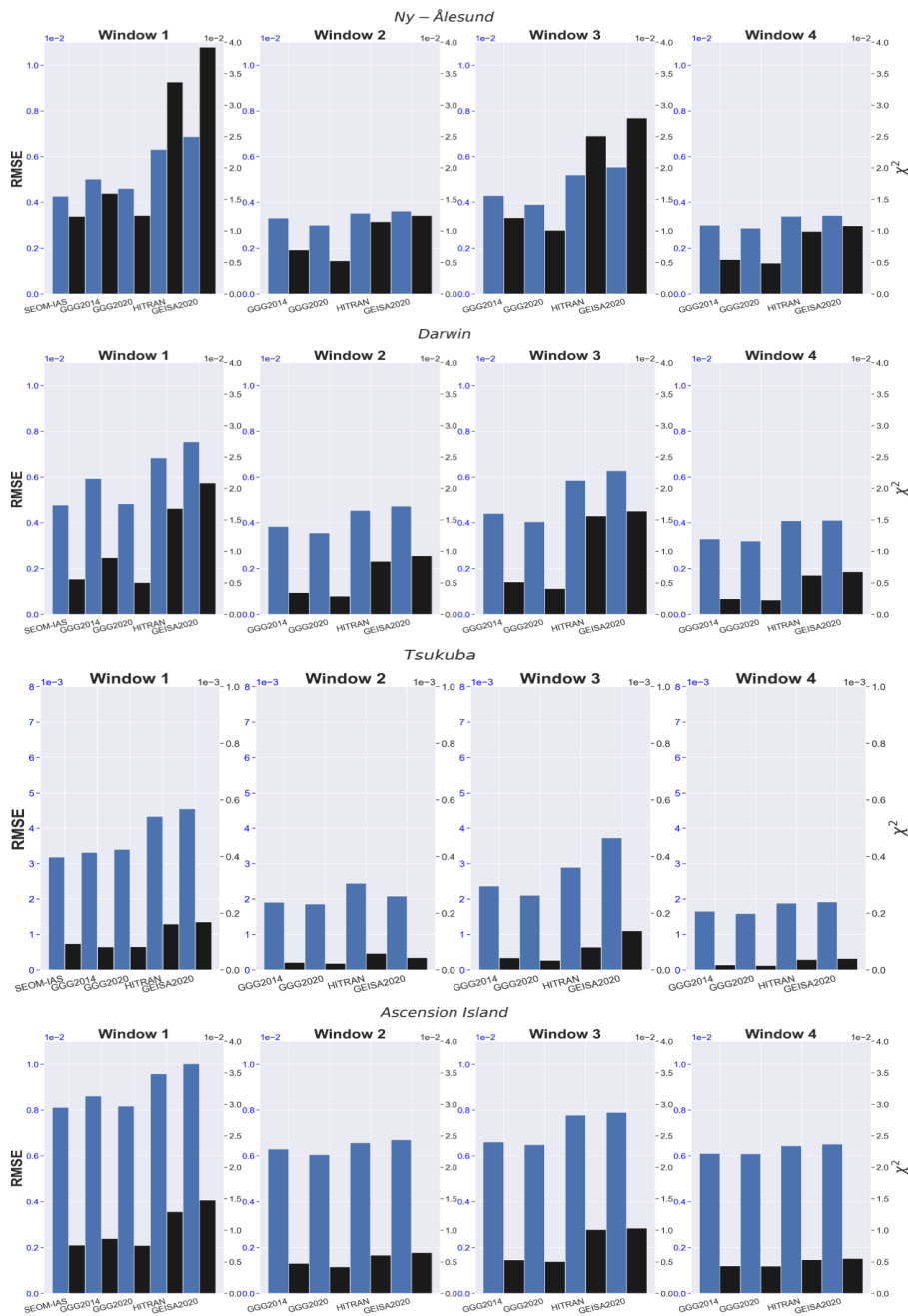
Figure 2. Bar chart indicating the fit statistics for a selection of retrievals from each of the TCCON site. Each row of the figure refers to results from each of the TCCON sites, indicated by the row title. Each column shows the results from each window, indicated by the title of each column. Each subplot shows the RMSE and χ^2 values for each spectroscopic database indicated in the x-axis, with the blue bars referring to the RMSE values, with magnitudes shown on the left-hand y-axis. The black bars refer to the χ^2 values, with the magnitudes indicated on the right-hand y-axis. Note the scale on the Tsukuba row is slightly different, to account for the lower magnitude results. A cross section of 500 spectra for each TCCON site are used to generate the statistics in this figure.

300   Since all trace gases are fitted simultaneously in all of the windows, there are no specific metrics associated with $^{13}CH_4$. $^{13}CH_4$ in this study is fitted in windows 1 and 4.

Building on the residuals indicated in Fig. 1, we investigate the differences observed in transmission residuals. We calculate the percentage difference for each spectroscopic database, w.r.t the tranmissions calculated by the GGG2014 database, for $^{12}CH_4$ and H_2O species.

Ny − Ålesund
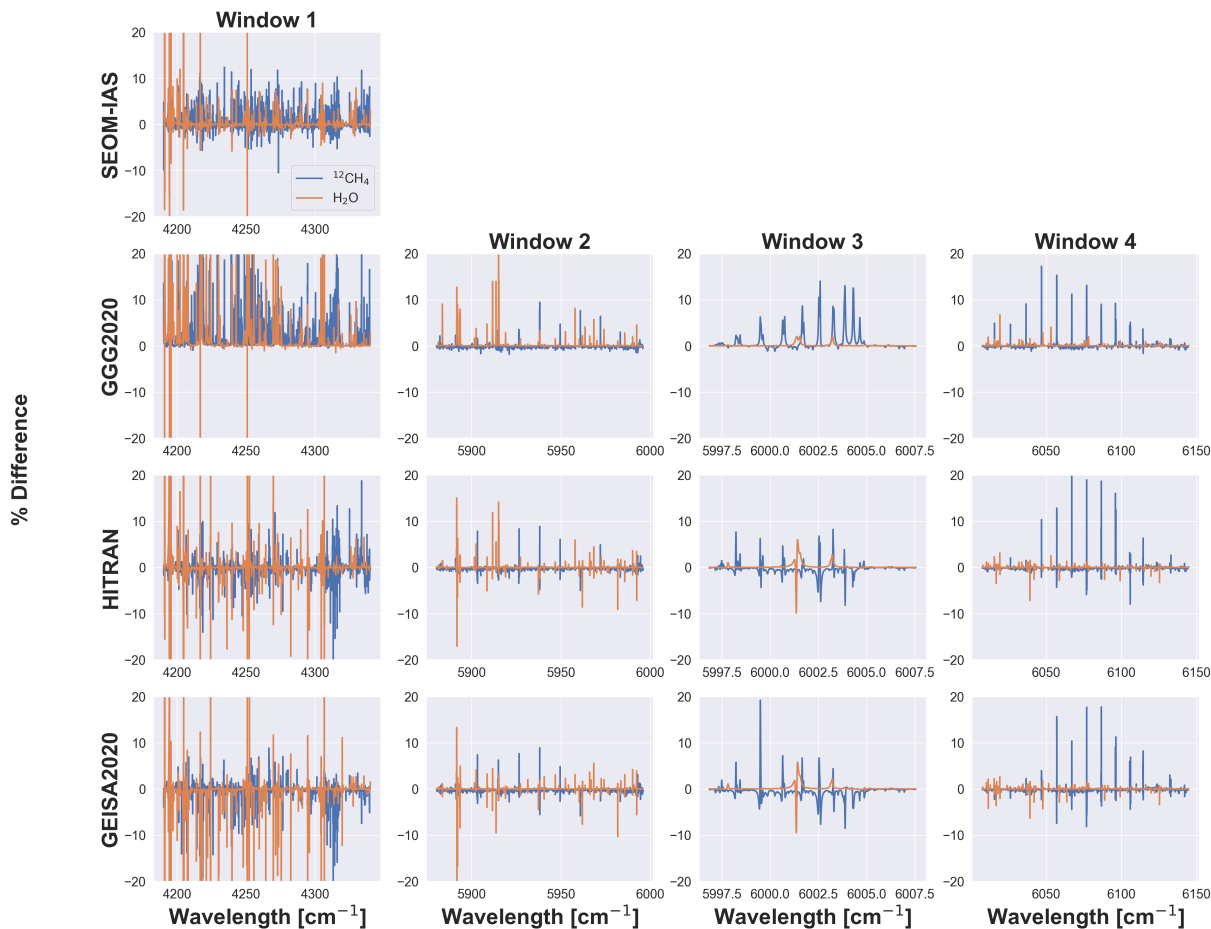
Figure 3. Percent difference in calculated transmission for $^{12}CH_4$ and H_2O from each spectroscopic database for each window w.r.t. GGG2014. Rows indicate spectroscopic database and columns indicate the windows. The y-axis values have been limited to 20% to avoid the plots being dominated by large excessive noise values, note however, especially in window 1, the values are sometimes in excess of 20%

305   The results shown in Fig. 3 suggest a number of different conclusions. Firstly the impact of differences in the spectroscopic parameters of water vapour are highly significant in window 1, more so than differences in $^{12}CH_4$, with each spectroscopic

database showing differences >20% at numerous wavelengths. Further, each spectroscopic database shows significant disagreement as to where the differences occur, suggesting large differences in the treatment of water vapour parameters in window 1 for each spectroscopic database. Therefore the poorer fit quality shown in Fig. 1 for window 1, is likely driven by water vapour uncertainty as opposed to methane. For window 2, we note again that water vapour seems to have the largest uncertainties (not to the degree of window 1). The main points of disagreement in general line up with the largest deviations in Fig. 1. For windows 3 and 4, water vapour differences have less impact, with the majority of the differences attributed to $^{12}CH_4$, which still have a lower magnitude than window 1. The large uncertainty in window 3 at 6001 cm^{-1} (characteristic bump shape), seems to be caused by water vapour uncertainty in HITRAN and GEISA2020. The main conclusion from this assessment, is that when considering uncertainty in $^{12}CH_4$ between windows and spectroscopic databases, uncertainty in water vapour should be considered at the same time.

3.2 Quantification of variance between windows and databases

The entire time series available for this study for each TCCON site are shown in Figs. 4, 5, 6 and 7. XAir, a quantity normally retrieved with TCCON is shown as an additional quality indicator for GGG2014, GGG2020, HITRAN and GEISA2020 (SEOM-IAS does not have spectral coverage in the TCCON XAir retrieval window) with variations between 0.96 and 1.04 assumed as good quality. Qualitative inspection of these figures shows scatter between all windows for each database, further the HITRAN, GEISA and SEOM-IAS databases show significant positive bias w.r.t. the standard deviation of the reference TCCON retrieval, indicated by the dashed black lines. Quantitative metrics for these figures are shown in Fig 8. We also find the XAir values indicate quality retrievals, with only a small number falling outside the acceptable range.
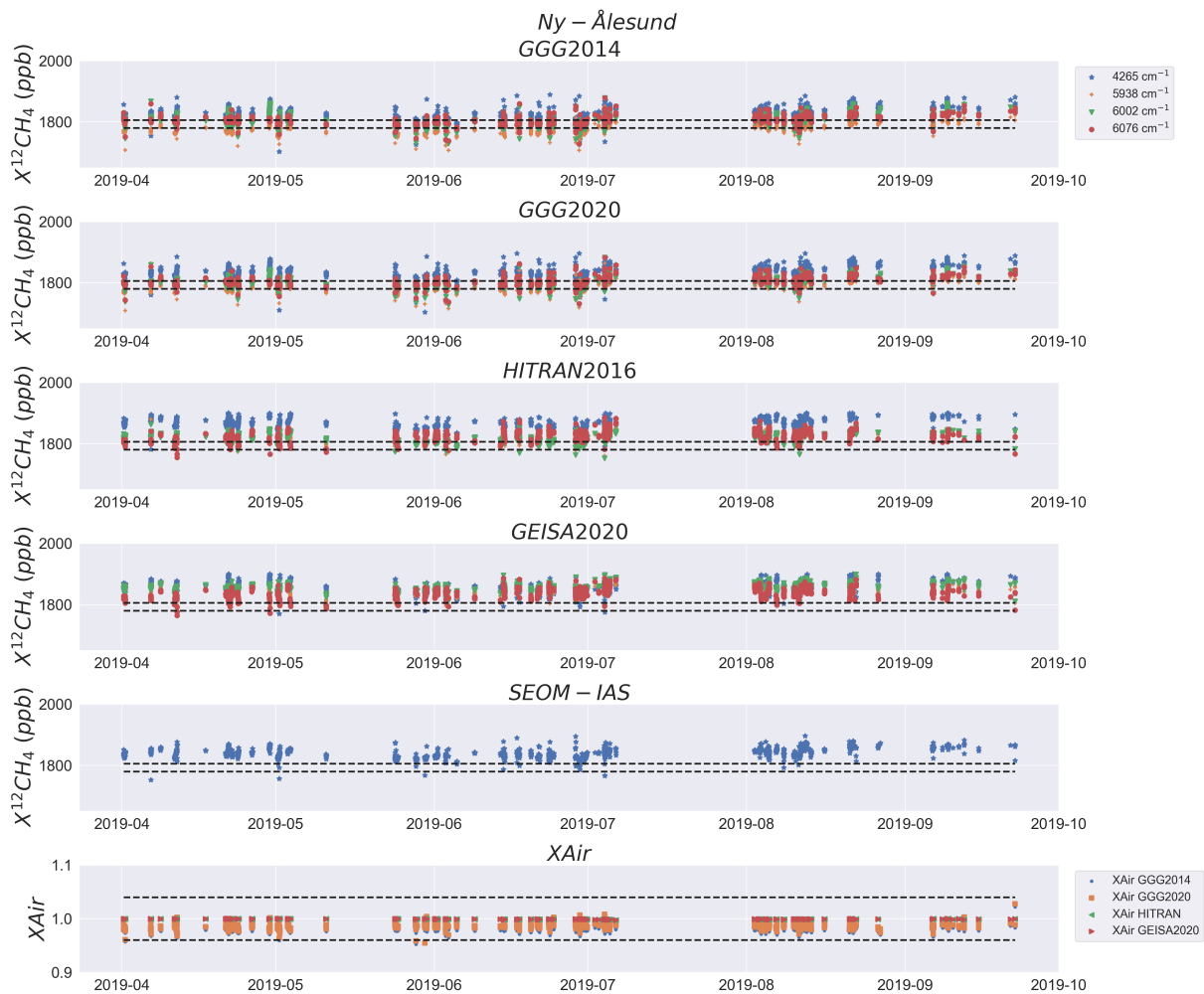
Figure 4. Retrieval time series for $^{12}CH_4$ DMFs from the Ny-Ålesund site. Each panel indicates retrievals from each spectral window (indicated in the legend) from a specific spectroscopic database, indicated in the panel title. Blue stars show retrievals from band 1, yellow pluses are band 2, green triangles are band 3 and red circles are band 4. The standard deviation about the reference TCCON retrievals are indicated by the horizontal dashed lines. The bottom panel indicates the retrieved XAir DMF as a quality indicator for the retrievals, with the dashed lines indicating the standard range of acceptable XAir values.
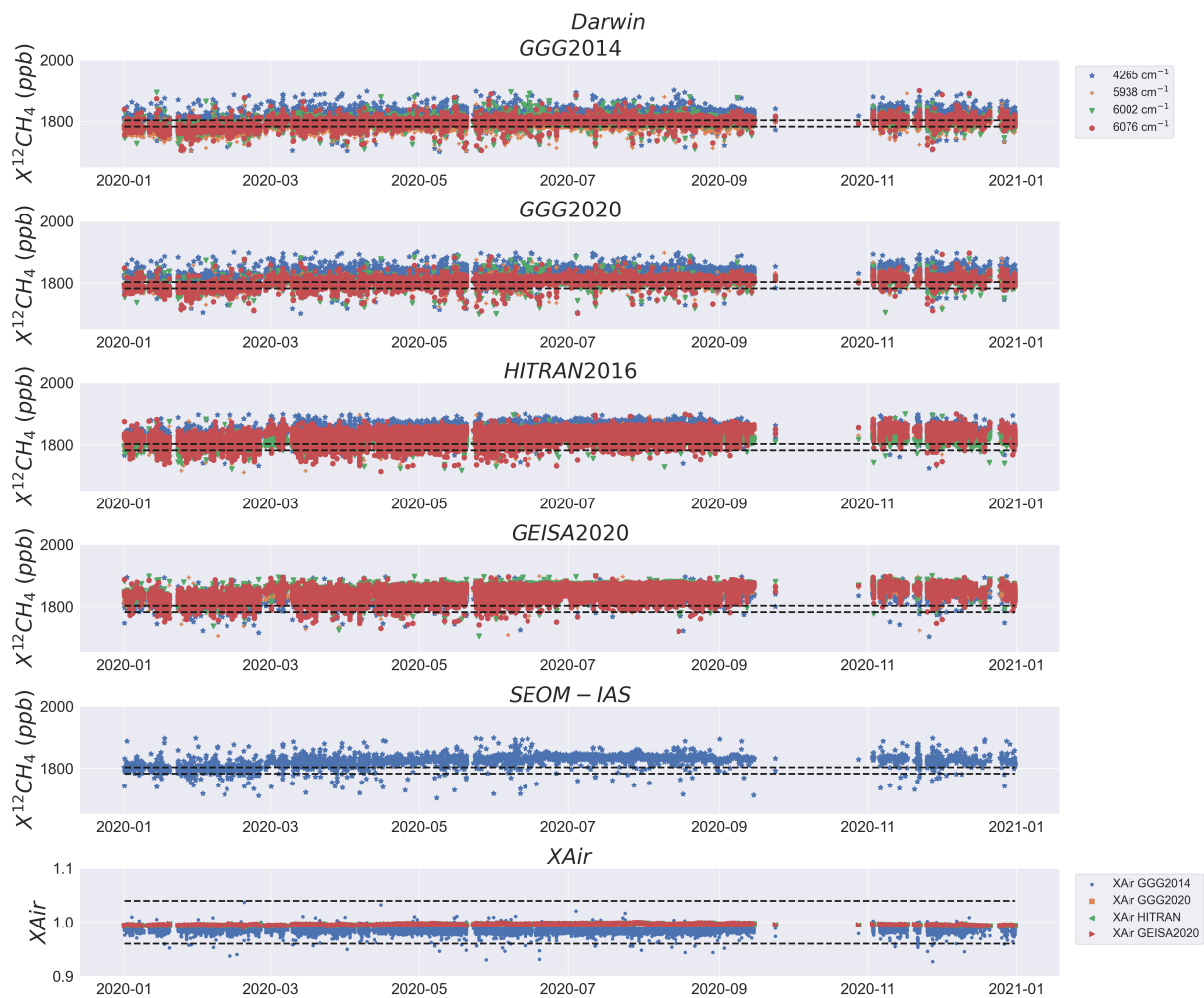
Figure 5. As Fig. 4, but for retrievals from the Darwin TCCON.
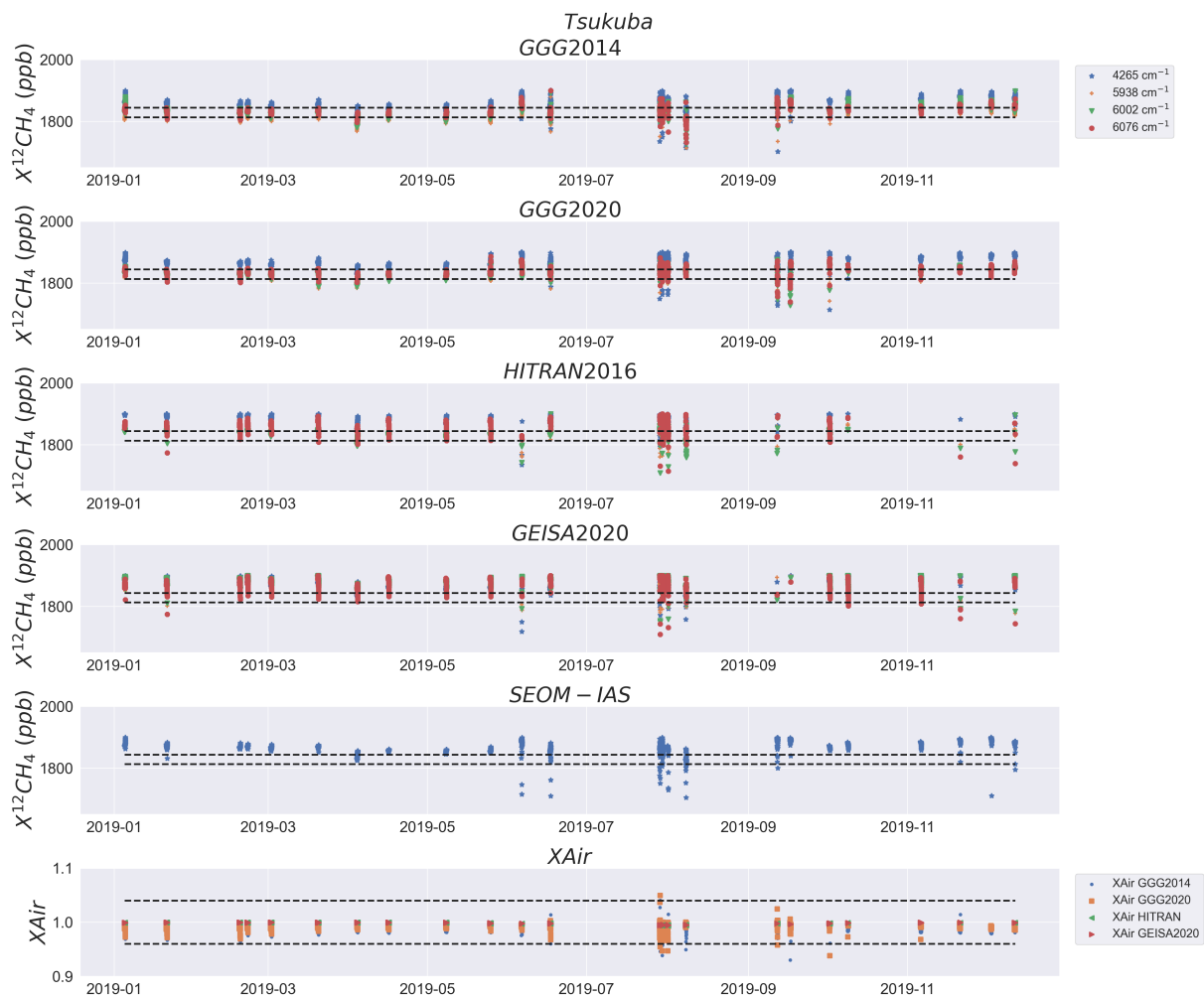
Figure 6. As Fig. 4, but for retrievals from the Tsukuba TCCON.
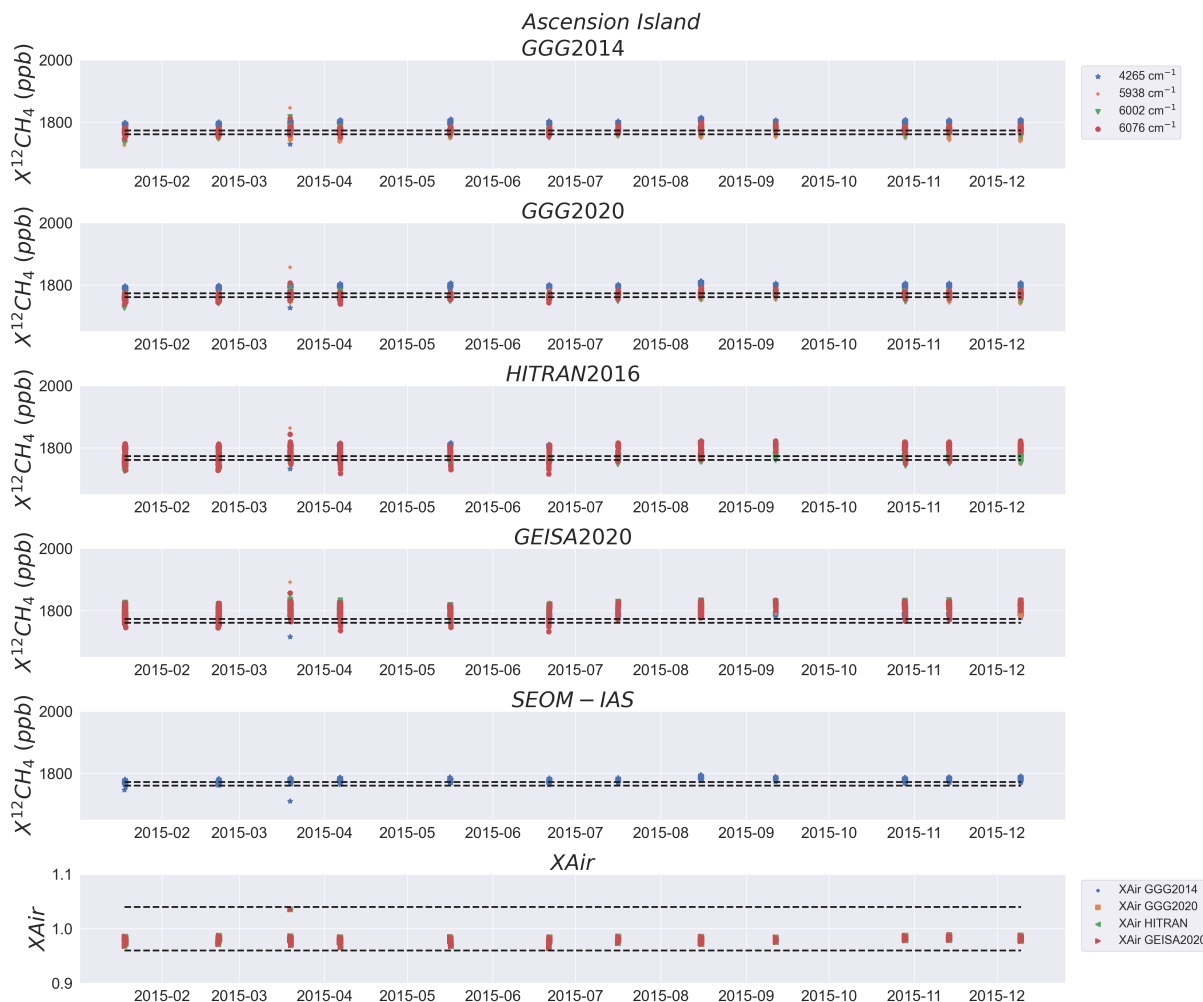
Figure 7. As Fig. 4, but for retrievals from the Ascension Island TCCON.

The metrics used in Fig 8 indicate that the bias for $^{12}CH_4$ retrievals for each database and window w.r.t the reference retrieval (Norm Abs Mean), and the presence of any large deviations (RMSE). These metrics are normalised by the retrieval uncertainty of the reference retrievals a weighted average of windows 2, 3 and 4 from GGG2014, thus we assume any biases with values greater than 1 cannot be attributed to uncertainty and are therefore real.

Firstly we analyse the results from Ny-Ålesund, which due to the constant nature of the atmospheric conditions can be considered as a baseline. For window 1, both the NRMSE and Norm Abs Mean values for all of the databases indicate values greater than 1, thus suggesting there are still significant variations in the treatment of spectroscopic parameters in window 1. The HITRAN and GEISA databases show bias deviations twice that of GGG2014, however these values do not indicate any one database is more accurate than the other, but either large differences in spectroscopic parameters or differences in sensitivity to local conditions. Windows 2 & 3 do not show any notable biases apart from the GEISA database which generally

335 shows the largest deviations across all of the windows (except window 1). In window 4, both HITRAN and GEISA show notable deviation from the reference retrievals, which is a surprising result given this window is popular in satellite retrievals of methane (Yoshida et al., 2013). We note the NRMSE and Norm Abs Mean values are similar in the majority of cases, indicating that there is an underlying bias between the database retrievals as opposed to large spikes of differences. Considering the bias deviations across the windows, GEISA is the only example to exceed values of 1 across all windows, with window 3 showing

340 the largest deviation from the reference value.

Secondly considering the dataset from Darwin, the magnitude of the NRMSE and Norm Abs Mean values are typically lower than the equivalents in the Ny-Ålesund dataset. The relative differences between the NRMSE and Norm Abs Mean values between the databases are the same as those shown in the Ny-Ålesund dataset, i.e. GGG2014 shows the lowest differences and GEISA shows the largest, apart from window 1 in which case it is HITRAN. Investigating each window in turn, only HITRAN

345 shows a notable deviation from the standard retrieval in window 1 with GGG2020 and GEISA not indicating a significant deviation above the standard noise level (only 0.02 and 0.07 above 1 respectively). For windows 2 & 3, only the GEISA database shows a significant bias with respect to the standard, as with Ny-Ålesund site. Again in window 4 only the HITRAN and GEISA databases show notable deviation from the standard, again suggesting the spectroscopic parameters in window 4 still have significant uncertainty w.r.t windows 2 & 3. The implication of the Darwin results w.r.t those from Ny-Ålesund are

350 that either or both the differences in the instrument setup and the local conditions impact inter-window/spectroscopic database biases. Note for the Darwin retrievals there is an inconsistency at the beginning of March 2020, where there is a small 'bump' in the magnitudes, and lower magnitude results are not apparent. This effect only appears at the start of March, and the typical retrieval variability is quickly restored. Quality control indicators (such as XAir) do not indicate any problems with the results in this period, and the reason for this inconsistency remains unclear.

355 The results for the Tsukuba retrievals are very similar to those shown for Ny-Ålesund, with GGG2014 not showing any significant differences except in window 1, as with the other sites HITRAN shows deviation in windows 1 and 4, and GEISA showing the largest differences apart from in window 1. However, the main difference is with the GGG2020 database, as with the other TCCON sites the normalised absolute mean shows deviation in windows 1 and 4, however the NRMSE indicates significant differences in all windows, suggesting there are a small number of retrieval cases that have large biases w.r.t the

360 standard values. This behaviour is not replicated in the other TCCON sites.

Finally, all results from the Ascension Island measurements indicate no deviations of any significance, contrasting with the results from all other sites. We note the standard deviation about the reference TCCON retrievals in Fig 7 is smaller than any of the other TCCON sites. This suggests constant retrievals in methane over the course of the year at Ascension Island, and therefore limited opportunity for biases to form.

365 The results in Fig 8 clearly indicate that in the cases where deviations exist, they are reflected in all of the TCCON sites (when significant), implying that despite the fit differences shown in Fig 2 these biases cannot (purely) be attributed to errors in the TCCON instruments, but given the consistency of the deviations we can attribute these differences to spectroscopic parameters. Figure 8 indicates that there are significant differences between SEOM-IAS, GEISA and HITRAN databases w.r.t. the GGG databases, which show less deviation. This is not surprising since the reference values are based on GGG2014, and GGG2020

is built upon GGG2014, however this is not the case in window 1 where larger deviations are observed. This suggests that knowledge of spectroscopic parameters in window 1 is still not as settled as the other windows which have been routinely used in TCCON. It is difficult to assess all of the differences between the databases, due to the range of parameters used; there are some papers which describe the sources of the spectral lines for each of the databases (Brown et al., 2013; Jacquinet-Husson et al., 2016), but specifics are limited due to the size of the databases. Complexity is added by the fact that several of these databases state that data is drawn from the same sources (Albert et al., 2009; Nikitin et al., 2015, 2017), however these papers go on to say that not all of the lines from these studies are implemented based on in house assessments of fit quality. The implication being that it is challenging to specifically identify where spectroscopic parameter differences occur between the databases.
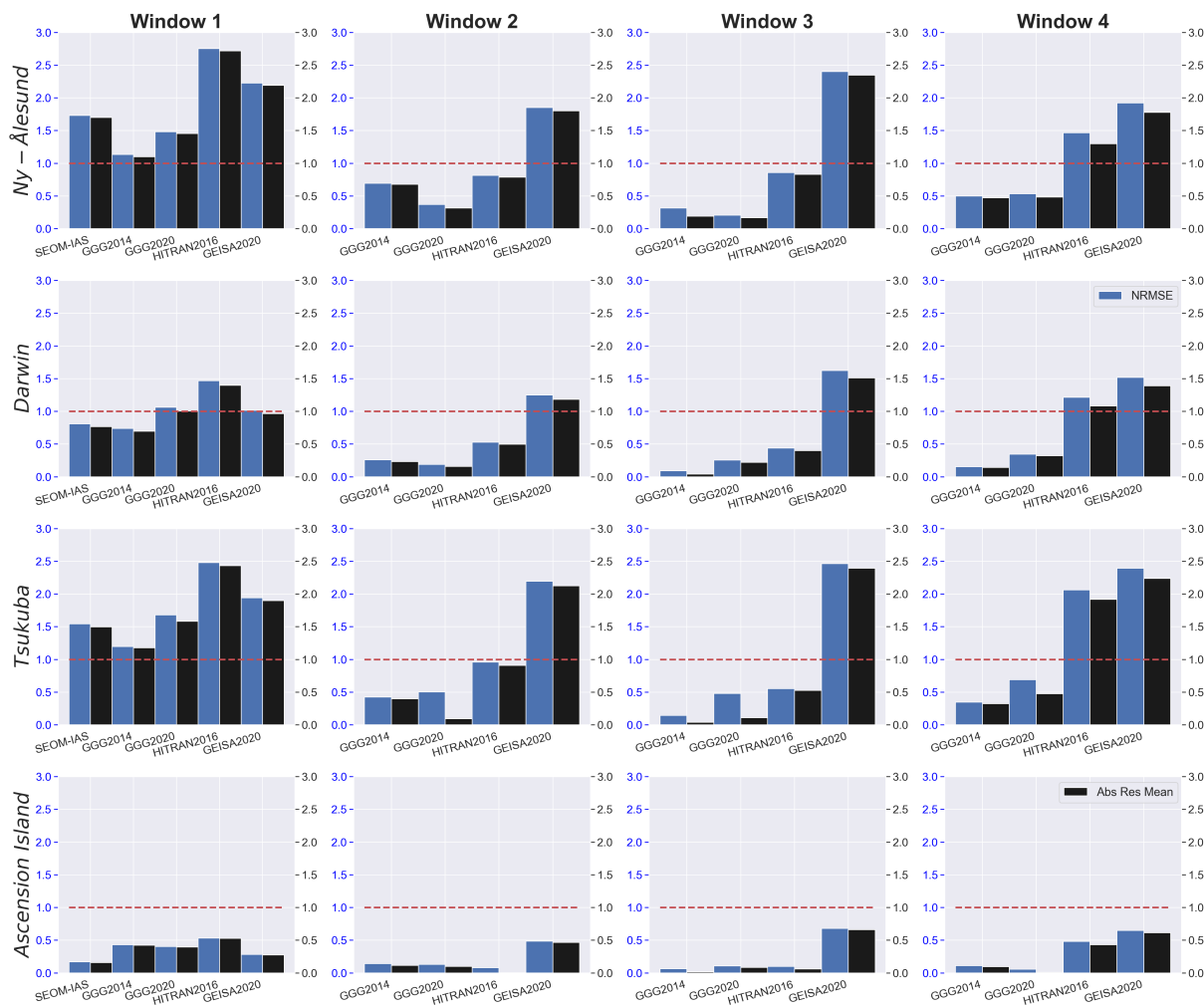
Figure 8. Bar plot indicating NRMSE and Normalised Absolute mean residual difference values for $^{12}CH_4$ retrievals from each TCCON site, each window and each spectroscopic database under consideration in this study with respect to the original TCCON methane retrieval window. Each row shows data from each TCCON site, as indicated by the y-axis titles, and each column shows results from each window, as indicated by the column title. Each subplot shows the NRMSE (the blue bars, magnitude shown by the left-hand y-axis) and Abs Res Mean (the black bars, indicated by the right-hand y-axis) values for each spectroscopic database as indicated by the x-axis. The horizontal red-dashed lines indicated the magnitude of 1, the value where we assume the bias values to be significant.

For $^{13}CH_4$ DMFs there is no obvious reference value available, since $^{13}CH_4$ is not typically retrieved from TCCON. We
380 therefore chose to use GGG2014 window 1 as a reference in order to investigate window deviations. We found that apart from
SEOM-IAS window 1 which showed deviation below the noise level from every TCCON site, every other case showed notable
levels of deviation ranging from 1.5-5. Here we cannot attribute these disagreements purely to spectroscopic differences since
$^{13}CH_4$ retrievals will be subject to high noise levels.

3.3 Impact of local condition changes on variance between windows and databases

385 It has been shown (Wunch et al., 2011) that the variability of local conditions can have an impact on the accuracy of TCCON retrievals (through the a priori data). We therefore investigate in this section if varying local conditions (specifically, water vapour, SZA and temperature) affect each window in each spectroscopic database differently. Wunch et al. (2011) identified a non-linear relationship between SZA and retrieval anomalies, we therefore fit the normalised residual DMF values with a second order model, to expose any potential non-linearity.
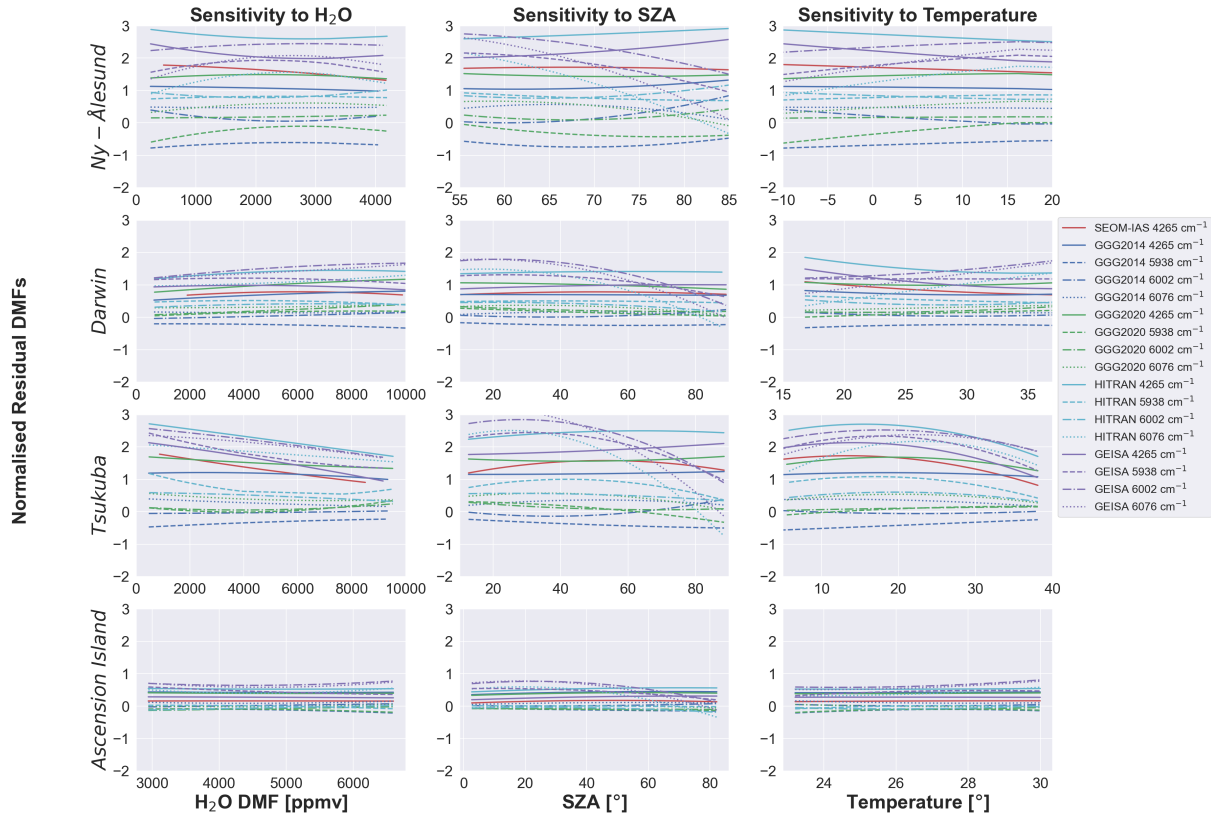
Figure 9. The sensitivity of water vapour, SZA and temperature variations on retrieved $^{12}CH_4$ DMFs from each TCCON site, spectroscopic database and windows. Each subplot shows the second order regression fit of the normalised residual between the retrieved window/spectroscopic database DMFs and the TCCON reference DMFs, with the fit window and spectroscopic database indicated by the legend. Each row of the figure shows data from each TCCON site as indicated in the y-axis, and each column shows the sensitivity to a specific condition as shown in the title.

390 Figure 9 qualitatively describes the sensitivity of each TCCON site/database/window to variations in local conditions. For Ny-Ålesund (row 1), there is a mixture of non-linear and linear sensitivities to variations in water vapour and SZA. Windows 2, 3 and 4 for GEISA2020 indicate particularly significant non-linear sensitivities to SZA variations. Sensitivities to temperature variation are generally linear, although some indications of slight non-linear behaviour are apparent (GEISA2020). For Ny-

Ålesund there are some cases where little sensitivity is observed, e.g. HITRAN, suggesting a wide range of responses in the databases/windows. In contrast to Ny-Ålesund, Darwin (row 2) shows limited sensitivity to local condition variations, with low magnitude linear gradients observed for most cases. There are some exceptions, notably HITRAN window 3 and GEISA2020 windows 3 and 4 in relation to SZA variations, where significant non-linear behaviour is observed. Tsukuba (row 3) again shows significantly different behaviour, with almost all databases/windows showing significant linear or non-linear sensitivity. Window 1 for SEOM-IAS, GGG2020, HITRAN and GEISA indicate significant negative linear relationships, with all other cases showing a range of sensitivity. For variations in SZA, as with Ny-Ålesund and Darwin, HITRAN window 3 and GEISA2020 windows 3 and 4 suggest strong non-linear sensitivity to variations in SZA. Most of the other windows/databases indicate some linear/non-linear sensitivity, but not to the same degree as HITRAN window 3 and GEISA2020 windows 3 and 4. Temperature variations for Tsukuba indicate significant non-linear sensitivity for window 1 in most cases (except GGG2014), and in general show different results from those shown in Ny-Ålesund and Darwin. Finally for Ascension Island, we note almost no sensitivity to any local condition variation, except for HITRAN window 3 and GEISA2020 windows 3 and 4 with SZA variations, which have shown sensitivity in all cases.

The qualitative assessment above is explored quantitatively in more detail in Figs 10, 11, and 12. Where the Pearson's correlation coefficients and the regression coefficients for a second order fit are shown. Note that the y-axis scales are unified for all sites and windows for each variable considered, to allow for direct comparison. In the following analysis, we assume the presence of a substantial linear correlation when r values > 0.5 are shown. Further, we assume any deviation from zero of the regression statistics to be the presence of at least minor sensitivity. First considering the impact of SZA variations in window 1 across all sites. There is no indication of a substantial linear correlation, with no database at any of the sites showing an r value > 0.5. The regression statistics for Darwin and Ascension Island do not suggest any non-linear or linear relationships, while Tsukuba indicates the presence of a non-linear relationship for SEOM-IAS and HITRAN. All three sites do indicate the presence a constant bias (although minor in the case of Ascension Island). The results from Ny-Ålesund indicate more significant sensitivity to SZA variations. SEOM-IAS shows a slight linear relationship, while GGG2014, GGG2020 and GEISA2020 show second and first order sensitivity, in contrast HITRAN shows only minor sensitivity. For window 2 we see weak to strong linear correlation in all databases across all sites, except for a few cases (e.g. HITRAN at Darwin and most cases at Ascension Island). The regression statistics indicate minor sensitivity for GGG2014, GGG2020 and HITRAN at most sites, except for Tsukuba where HITRAN is significant. Ny-Ålesund shows significant non-linear regression statistics for all databases, indicating significant sensitivity to SZA variations, and given that Ny-Ålesund operates at the highest SZAs of all of the TCCON sites under consideration, this is logical. Window 3 shows notable levels of correlation to SZA variations w.r.t. all sites, with Ny-Ålesund, Tsukuba and Ascension Island showing particularly large correlations (>0.5), especially in the GGG2014 and GEISA2020 databases. However, Darwin and Ascension Island show only very minor sensitivty to SZA variations, except for GEISA2020 at these sites. Tsukuba and again Ny-Ålesund shows much higher sensitivity for all databases (except GGG2020 and HITRAN for Tsukuba), with the regression statistics showing 2nd and 1st order coefficient values much larger than any other case. Window 4 shows large linear correlations for almost all of the databases, in the Ny-Ålesund retrievals especially. Generally for Darwin, Tsukuba and Ascension island, little to no sensitivity to SZA variations are observed for

GGG2014 and GGG2020, while HITRAN and GEISA2020 all indicate more significant sensitivity, comparable to Ny-Ålesund in window 1. In contrast, Ny-Ålesund shows a much greater sensitivity to SZA variations for all spectroscopic databases. Overall the results in Fig 10 indicate limited to no sensitivity to SZA variations for the Darwin, Tsukuba and Ascension Island sites for the GGG2014 and GGG2020 databases, while HITRAN and GEISA2020 do indicate some sensitivity, especially in windows 3 and 4. The Ny-Ålesund site, however, shows significant sensitivity for all of the spectroscopic databases, across all of the windows. With no clear 'winner' or 'loser' in terms of windows and spectroscopic databases, with all statistics showing similar results. These results could be explained by the fact that Ny-Ålesund operates at higher SZA angles than any of the other TCCON sites, meaning the retrieval path length will be longer, potentially allowing for more errors to propagate into the retrievals. The results from Ascension Island, which operates at lower SZAs than any of the other TCCON sites considered in this study indicates the lowest magnitude sensitivities, adding weight to this argument.

The sensitivity of each window to water vapour variation is explored in Fig 11. Beginning with window 1, only the SEOM-IAS, HITRAN and GEISA2020 databases at the Tsukuba site indicate the presence of a significant linear correlation. For these sites we note that the second order regression statistics indicate only very minor sensitivity, and although there is more evidence of stronger first order sensitivity, the lack of a linear correlation suggests water vapour variation only has a minor impact. Except at Tsukuba which is an interesting results, given both Tsukuba and Darwin both have large variations in background water vapour. Ny-Ålesund however, indicates the presence of strong non-linear relationships for GGG2020, HITRAN and GEISA2020, contrasting the results from the other sites. Window 2 shows little linear correlation for most of the cases, except for GGG2020 at Ny-Ålesund, and all sites at Tsukuba. Ny-Ålesund indicates the presence of significant non-linear correlations for all spectroscopic databases in contrast to Darwin which shows only very minor sensitivity to water vapour variations. GGG2014 at the Tsukuba site presents a very minor linear sensitivity, while HITRAN and GEISA2020 both show the presence of a significant non-linear regression. Finally for window 2, Ascension Island shows similar results for GGG2014, GGG2020 and HITRAN, namely a minor non-linear relationship, while GEISA2020 shows the presence of a more significant non-linear relationship. With window 3, there are no cases of significant linear correlation; we note no or very slight (HITRAN and GEISA2020 Darwin) non-linear relationships at Darwin, Tsukuba and Ascension Island, except for GEISA2020 at Ascension Island. The results from Ny-Ålesund contrast the other sites, by indicating strong non-linear relationships for all spectroscopic databases, except GGG2020. Window 4 shows similar results to window 3, with almost no cases indicating significant linear correlation (except GGG2014 at Tsukuba). Darwin and Tsukuba show only very slight non-linear sensitivity to water vapour variation, while Ny-Ålesund and Ascension Island both indicate significant sensitivity across all databases (aside from GGG2014 at Ny-Ålesund). The conclusions from this analysis suggests locally varying conditions are key in determining the impact of water vapour variations. It is interesting that the site with the lowest magnitude background water vapour (Ny-Ålesund) is the most affected by water vapour variation, as opposed to Darwin which has the highest background and variation, which shows little sensitivity to water vapour variation. The key difference between Ny-Ålesund and the other sites is the SZA at which measurements are taken, meaning TCCON measurements taken at high SZA will be more sensitive to other varying conditions.

The results for retrieval bias sensitivity to variations in temperature are shown in Fig 12. For window 1, only the Tsukuba site shows significant linear correlation with temperature variation, for the SEOM-IAS, HITRAN and GEISA2020 databases. Ny-Ålesund shows limited sensitivity across all spectroscopic databases, contrasting with the other TCCON sites, all of which indicate some sensitivity. Darwin and Tsukuba show the presence of a non-linear relationship across all spectroscopic databases, with Ascension Island showing a non-linear relationship in most cases. For window 2, Ny-Ålesund shows very limited non-linearity, and although strong linear correlations are observed, only linear coefficients of minor magnitude are observed, indicating low sensitivity. Darwin shows little to no sensitivity across all cases, while Tsukuba suggests a strong linear correlation for GGG2014, but almost no sensitivity, but both HITRAN and GEISA2020 suggest strong non-linear relationships. Contrasting the other sites, Ascension island shows almost no linear correlation, but the presence of significant non-linear relationships for all spectroscopic databases. For window 3, Ny-Ålesund shows only minor sensitivity to temperature variations, while Darwin indicates the presence of non-linear relationships similar to window 1. Tsukuba shows similar results to window 2, such that GGG2014 does not indicate any sensitivity, while HITRAN and GEISA2020 show stronger non-linear relationships. Again Ascension island is the outlier, showing strong non-linear sensitivity for all spectroscopic databases. Window 4 is also different from the other windows, with the results from Ny-Ålesund generally showing more sensitivity to temperature variations than the other windows, especially GEISA2020. For Darwin, GGG2014 and GGG2020 show very little sensitivity, while HITRAN and GEISA2020 show significant non-linear relationships. Tsukuba shows similar results to windows 2 and 3, where HITRAN and GEISA2020 indicate strong non-linear sensitivities, while GGG2014 is largely invariant to temperature variations. Ascension Island shows similar results to windows 2 and 3, where strong non-linear relationships are observed for all spectroscopic databases. In summary, variations in temperature will impact inter-window and inter-database biases, the impact depends significantly on the local conditions as well as the window and database in question. We note that Ascension Island shows the most significant impact in these results, however this is possiblly a biased result due to the fact that Ascension Island shows very little temperature variation over the measurement dataset. The other sites, which capture measurements over a much wider range of temperatures are therefore more reliable.

In general, there is no clear case of one window or database showing clear sensitivity over and above than any of the others (although Ascension Island is typically less sensitive). However there are clear indications of sensitivity to variations in the local conditions which vary between window, database and TCCON site, in some cases very strong correlations and sensitivities. For example, Ascension Island has some of the least varying conditions of all of the sites, and the results from this study indicate the least bias sensitivity. While Ny-Ålesund has less variability than Darwin or Tsukuba, but takes measurements under more challenging conditions, and also shows more sensitivity than either of these sites.

We note when calculating the Pearson's correlation coefficient for GGG2020 values for window 1 at the Tsukuba site, large 'p' values were found, indicating these results are not statistically significant, and therefore should be ignored. The p-test was applied to all other window and spectroscopic database combinations, all showed significance w.r.t the p-test i.e. $\ll 0.05$.
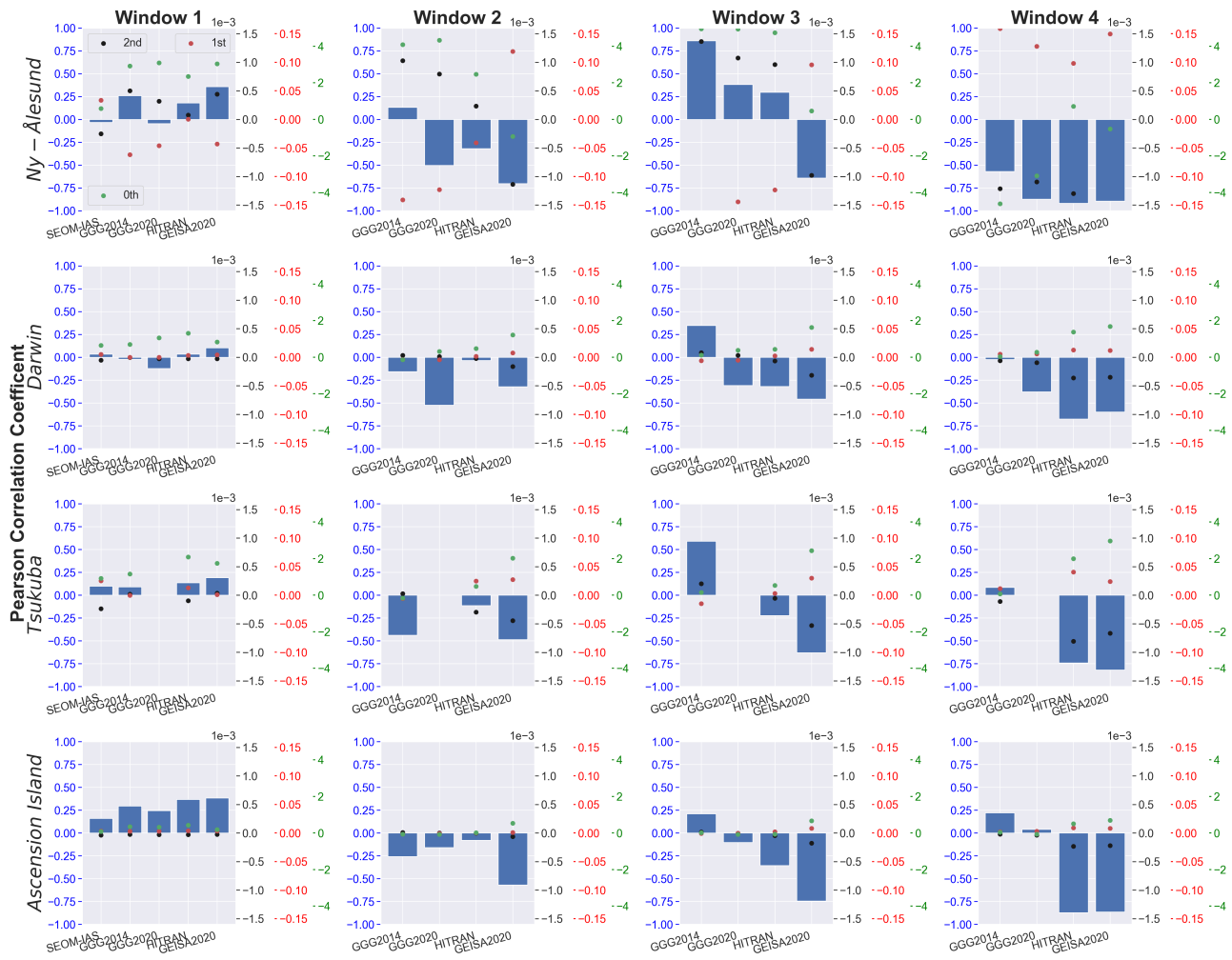
Figure 10. Bar and scatter chart indicating the statistics behind the sensitivities to SZA variations shown in Fig 9. Each row indicates the results from a TCCON site, as indicated by the y-axis label, each column shows the results from a particular window as shown by the column title. The blue bar plot show the Pearson correlation coefficient, with the left-hand blue y-axis values the appropriate scale. The black dots show the second order coefficient from the regression from the fits shown Fig 9, with the right-hand black y-axis values as the scale. The red dots show the first order coefficient, corresponding to the right-hand red y-axis, and the green dots show the constant values corresponding to the right-hand green y-axis. Note all values for GGG2020 at the Tsukuba site have been removed due p-test failure.
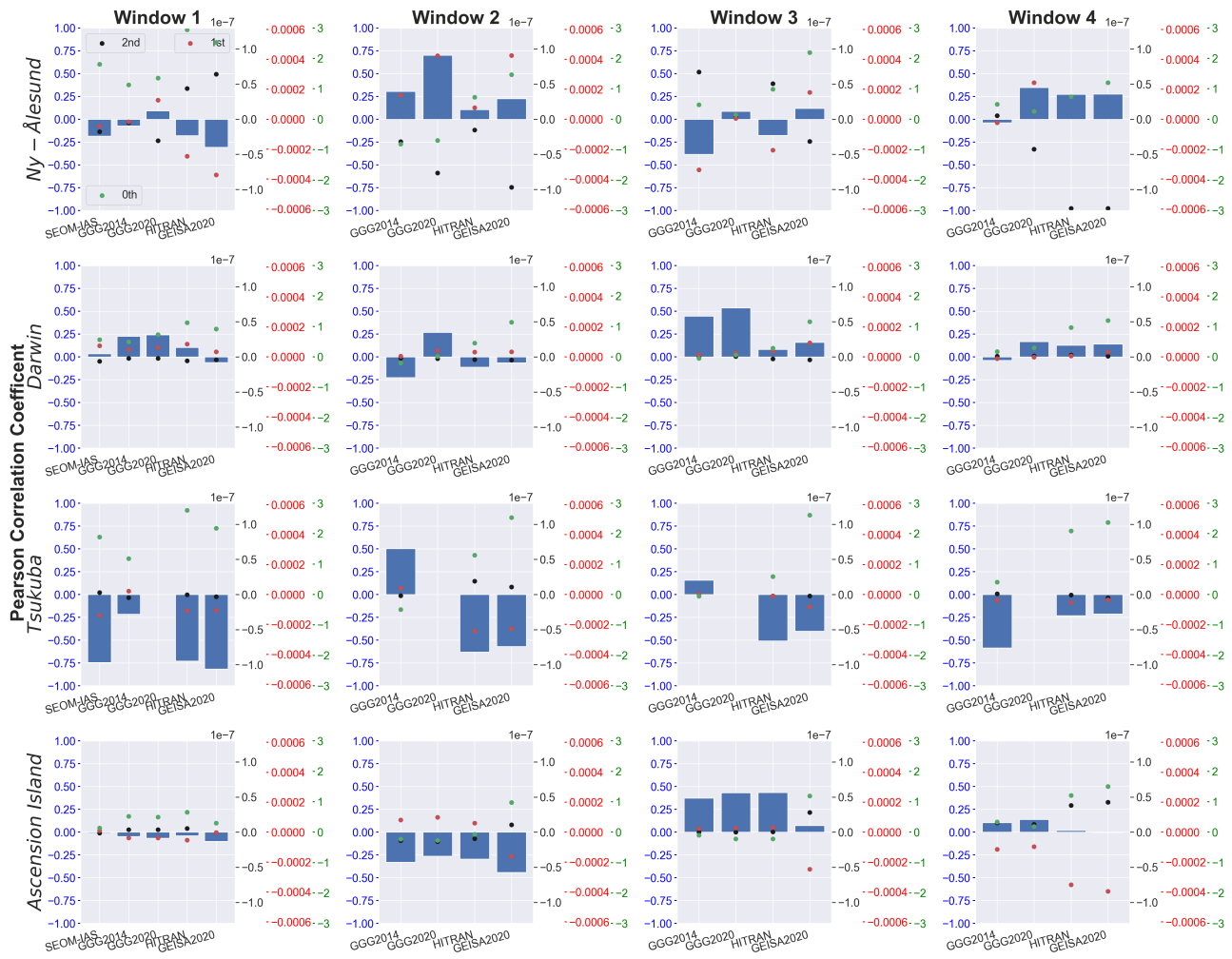
Figure 11. As Fig 10, but showing the sensitivities to water vapour variations.
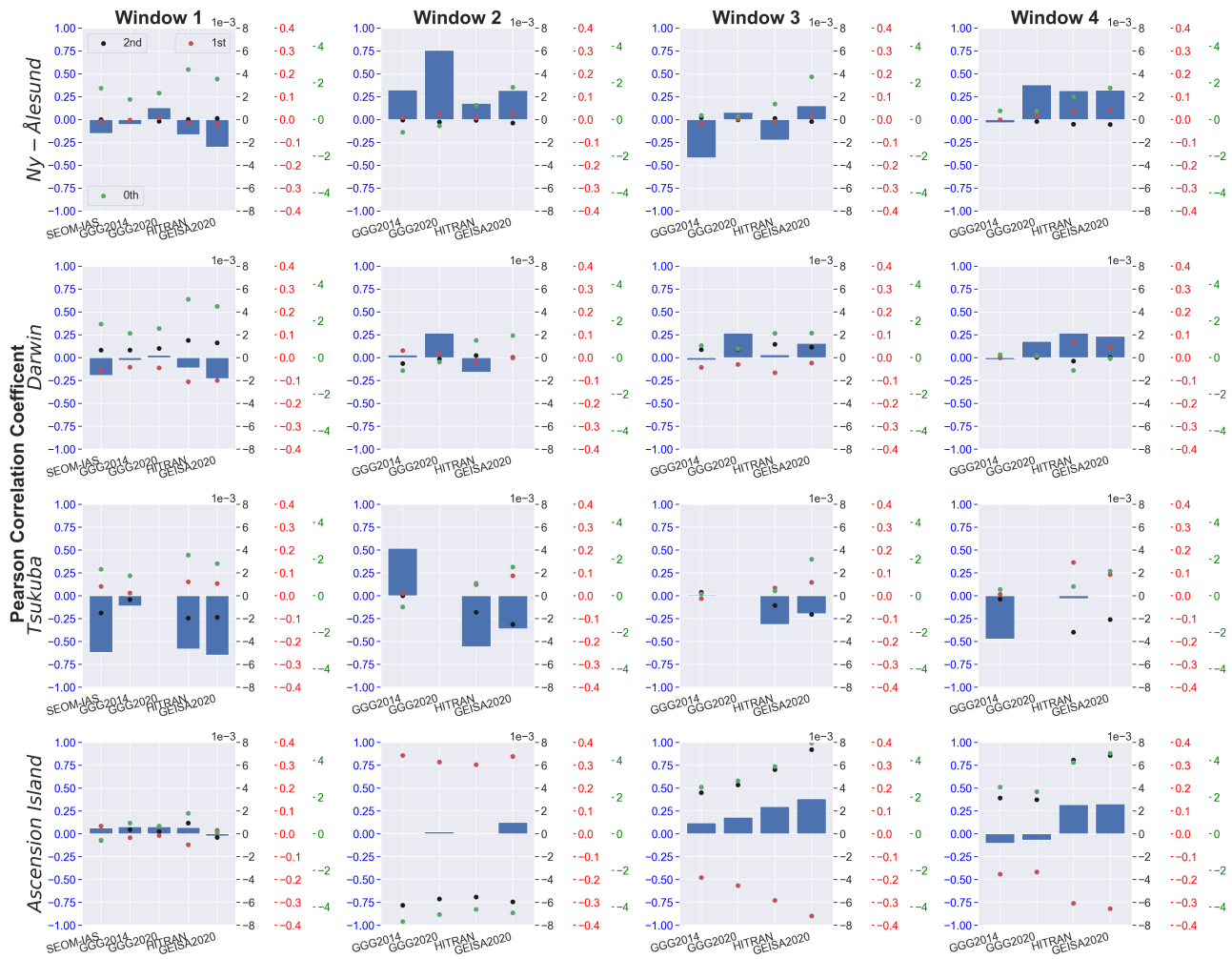
Figure 12. As Fig 10, but showing the sensitivities to temperature variations.

A similar analysis for retrieval bias sensitivities for $^{13}CH_4$ indicated high levels of sensitivity to SZA variation, especially those retrievals from Ny-Ålesund where SZAs are high. There are some windows that indicate no correlation, but the majority had values greater than 0.3. W.r.t water vapour and temperature variation, these results are mixed with different windows and databases at different sites indicating different results. However there is a general trend of sensitivity to water vapour and temperature variations, with only a small number of cases indicating no correlation. These results suggest $^{13}CH_4$ retrievals are more sensitive to changing conditions than $^{12}CH_4$, which is the expected result.

3.4 Calculation of $\delta^{13}C$ values

The calculation of the $\delta^{13}C$ values (Eq 1), can give some insight into the accuracy of $^{13}CH_4$ retrievals from TCCON, as well as the impact of local condition variations on these retrievals. $\delta^{13}C$ is calculated for all TCCON sites using all combinations

of windows from all databases, using averaged $^{12}CH_4$ and $^{13}CH_4$ for the whole time series available for each TCCON site.
505 There are two factors to look for in the analysis of $\delta^{13}C$, firstly the bias w.r.t. the accepted atmospheric average of -47‰ and the consistency of the calculated values across databases and windows.

Table 4. Averaged values of $\delta^{13}C$ from all TCCON sites for all possible combinations of $^{12}CH_4$ with window 1 of $^{13}CH_4$ for each spectral database.

Site	Database	Windows 1 & 1	Windows 2 & 1	Windows 3 & 1	Windows 4 & 1
Ny-Ålesund	GGG2014	-102‰	-77.3‰	-89.5‰	-93.0‰
	GGG2020	-90.6‰	-66.1‰	-73.0‰	-77.1‰
	HITRAN	8.98‰	38.4 ‰	37.3‰	37.3‰
	GEISA	-66.4‰	-60.1‰	-67.6‰	-59.2‰
	SEOM	-91.3‰			
Darwin	GGG2014	-126‰	-107‰	-113‰	-63.0‰
	GGG2020	-78.1‰	-59.4‰	-60.8‰	-77.1‰
	HITRAN	-60.1‰	-39.9‰	-37.4‰	-52.1‰
	GEISA	-72.1‰	-76.5‰	-82.8‰	-80.2‰
	SEOM	-88.3‰			
Tsukuba	GGG2014	-125‰	-105‰	-109‰	-114‰
	GGG2020	-101‰	-81.8‰	-81.8‰	-86.1‰
	HITRAN	-52.7‰	-31.3‰	-26.3‰	-41.2‰
	GEISA	-71.1‰	-73.4‰	-76.7‰	-74.2‰
	SEOM	-77.3‰			
Ascension Island	GGG2014	-130‰	-113‰	-117‰	-120‰
	GGG2020	-89.3‰	-72.0‰	-72.6‰	-75.3‰
	HITRAN	-94.2‰	-76.1‰	-73.9‰	-90.5‰
	GEISA	-70.6‰	-77.1‰	-83.8‰	-82.1‰
	SEOM	-104‰			

Table 5. Averaged values of $\delta^{13}C$ from all TCCON sites for all possible combinations of $^{12}CH_4$ with window 4 of $^{13}CH_4$ for each spectral database.

Site	Database	Windows 1 & 4	Windows 2 & 4	Windows 3 & 4	Windows 4 & 4
Ny-Ålesund	GGG2014	2.46‰	29.7‰	16.1‰	12.2‰
	GGG2020	9.08‰	36.3‰	28.6‰	24.1‰
	HITRAN	-49.1‰	-21.3‰	-22.4‰	-27.2‰
	GEISA	-26.6‰	-20.0‰	-27.9‰	-19.1‰
Darwin	GGG2014	-117‰	-97.4‰	-103‰	-105‰
	GGG2020	-131‰	-114‰	-115‰	-117‰
	HITRAN	65.3‰	88.1‰	91.0‰	74.3‰
	GEISA	134‰	129‰	121‰	124‰
Tsukuba	GGG2014	-21.8‰	0.953‰	-4.12‰	-9.03‰
	GGG2020	-26.7‰	-5.62‰	-5.66‰	-10.3‰
	HITRAN	14.5‰	37.5‰	42.9‰	26.9‰
	GEISA	56.4‰	53.8‰	50.1‰	52.9‰
Ascension Island	GGG2014	-125‰	-107‰	-112‰	-115‰
	GGG2020	-140‰	-124‰	-124‰	-127‰
	HITRAN	11.5‰	31.8‰	34.3‰	15.6‰
	GEISA	87.4‰	79.9‰	72.0‰	74.0‰

Tables 4 and 5 indicates a wide range of results, suggesting either significant differences in spectroscopic parameters or large retrieval uncertainty. GGG identifies the mean uncertainty of $^{13}CH_4$ retrievals to between 0.5 - 2 ppb ($\sim$2.5-10%) depending on the database and TCCON site. However, given that these uncertainties can be averaged over a long period of time, they should reduce significantly (by $\sim$ x200 in the case of Darwin), meaning that the precision of $^{13}CH_4$ retrievals should be very high (e.g. <0.006 ppb). Therefore precision errors cannot explain the differences in $\delta^{13}C$ values shown in Tables 4 and 5, meaning differences in the spectroscopic databases are the key sources of errors in $^{13}CH_4$ retrievals. This therefore suggests that knowledge of $^{13}CH_4$ retrievals spectroscopic parameters must be improved before serious attempts at remote sensing of $^{13}CH_4$ can be made.

Looking at these results in more detail, considering the retrievals that use $^{13}CH_4$ from window 1, these combinations yield surprisingly consistent results site to site and window to window. Except for the HITRAN results which show significant bias at the Ny-Ålesund site, although this is contrasted by the HITRAN results at Darwin and Tsukuba which indicates values very close to what might be expected. Indeed, the results from HITRAN at Ny-Ålesund are significantly different from those at any of the other sites, which can be explained by $^{13}CH_4$ retrievals showing significantly larger biases (at least x2 any other database), and a very high Pearson's correlation (0.7). The results from GEISA are the most consistent across the window

combinations for all sites, showing a maximum of ∼13‰ variation across all window combinations which is a remarkable result. For comparison purposes, HITRAN shows ∼25‰ variation, GGG2020 ∼18‰ variation and GGG2014 ∼25-60‰ variation. The variations between databases in the same window combinations are larger than those in-between windows, suggesting variable dependence on local conditions, and thus differences in spectroscopic parameters. Except for HITRAN, all of the databases and windows seem to underestimate the accepted $\delta^{13}C$ values.

The results for the $^{13}CH_4$ window 4 combination are highly varied, more so than those shown for the window 1 combinations. For Ny-Ålesund both the GGG2014 and 2020 results show high levels of bias and significant variation, while the HITRAN and GEISA results show much lower bias levels and generally consistent results, with the HITRAN window 1 & 4 combination showing a realistic result. This is contrasted by the results from Darwin, where large biases are observed from all of the databases, but similar levels of consistency between the window combinations. Tsukuba again shows large bias levels between databases and windows, with GEISA showing high levels of consistency but large bias. Ascension Island shows similar results to Darwin (except for the HITRAN calculations), indicating similar sensitivity to background conditions. Pearson correlation coefficients for window 4 generally indicated lower levels of sensitivity to variations of local conditions than window 1, suggesting the spectroscopic parameters for $^{13}CH_4$ in window 4 have significant uncertainty. Furthermore, we found that the retrieval errors generated from $^{13}CH_4$ in window 4 were at least double those from $^{13}CH_4$ in window 1. This lower uncertainty is key in explaining the lower variation in $\delta^{13}C$ metric calculated using window 1.

Overall the results in Tables 4 and 5 suggest using GEISA2020 $^{13}CH_4$ retrievals from window 1 to calculate $\delta^{13}C$ values, showing high levels of consistency across all windows and sites, and relatively low bias levels. This consistency is surprising and is worth further investigation, however, Window 4 for all spectroscopic databases yield far less accurate results, suggesting more work must be done for spectroscopic parameters in this window for $^{13}CH_4$.

4 Discussion

We have shown the presence of correlations between variations in specific local conditions and retrieval biases in this paper, however it should be noted that other local conditions do vary in parallel with those indicated in Sect, 3.3. It is therefore likely that each window and spectroscopic database show bias variability due to the variation of a number of conditions simultaneously, which is why each TCCON site shows different results. The key message remains true however, that different windows in different spectroscopic databases are sensitive to varying degrees to local changing conditions. Further analysis in this topic should be assessed, for example the impact of the air-mass factor changes or variations in the O_2 retrievals may be important. We note Cygan et al. (2012); Ngo et al. (2013) identify Voigt broadening parameters for O_2 as insufficient. The release of the GGG2020 environment may allow for the testing of the impact of non-Voigt parameters on O_2 retrievals. Currently, the bias present in TCCON O_2 retrievals are removed by air-mass correction factors, based on results from the O_2 parameters in the GGG2014 database, and modified for each TCCON site. This means the use of DMFs for the comparisons in this study are likely to unfairly favour the results from the GGG2014 database. Therefore a potential option for comparison purposes would be to calculate volume mixing ratios (VMRs) based on dividing the retrieved methane quantity by the column

of dry air calculated using the surface pressure and water vapour column, as opposed to the O_2 column. While this method would remove the biases associated with the GGG2014 O_2, it would introduce biases associated with the measured surface pressure, and the water vapour column which are more significant than the biases associated with O_2 (Wunch et al., 2011). Further, one of the key reasons for using DMFs as opposed to VMRs is that O_2 is well known and a constant, and can be used as a standard between all of the sites. Therefore, while the use of DMFs introduces biases, the use of VMRs would make the different sites less comparable.

We have also not considered errors in the instruments themselves, for example variations in the instrument line shape function between different TCCON instruments could cause additional biases.

We note that advancements are currently being tested on retrievals of methane from TCCON spectra, for example with the "SFIT4" algorithm (Zhou et al., 2019), which allows for profile retrievals and would therefore be less subject to the methane profile errors that can occur in GGG retrievals (Wunch et al., 2011). In addition to profile retrievals, this study used the GGG2014 retrieval software, while the more recent version of this software GGG2020 has also recently been announced. This update includes an improved spectroscopic database (this database was used in this study, wrapped in the GGG2014 software), which includes non-Voigt line shapes for methane, and possibly other gases. However, the GGG2014 software used in this study cannot leverage the non-Voigt parameters currently embedded in the GGG2020 spectroscopic database. Therefore further analysis using the GGG2020 software instead of GGG2014, and the use of other algorithms in this study could yield improved or different results. However, it is likely that the bias problems identified in this study may remain to some degree.

In addition to understanding the biases associated with retrieving $^{12}CH_4$ DMFs from TCCON spectra with differing spectroscopic databases, this study touches on a question that is of some interest to the community, namely whether it is possible to calculate realistic and constant $\delta^{13}C$ values from TCCON. The results shown in Tables 4 and 5 suggest not this is not yet possible, since they are often significantly different from the tropospheric average $\delta^{13}C$ value which is assumed to be -47‰ (Sherwood et al., 2016), and variable between databases and windows. There are some interesting cases where results close to the expected $\delta^{13}C$ value are calculated (e.g. windows 1 & 1 for HITRAN at Tsukuba), however given the same database in the same windows yields a completely inaccurate result at another TCCON site, it is challenging to draw any conclusions without further analysis. What is clear however, is that the $\delta^{13}C$ values calculated using $^{13}CH_4$ retrievals from window 1 tend to have less biases than those calculated using window 4, and show less variation between windows and TCCON sites, as well as more consistent results between the spectroscopic databases. The implication of these results are that window 1 is superior to window 4 for retrieving $^{13}CH_4$ DMF, however whether this is due to superior information content, or more accurate knowledge of spectroscopic parameters requires further research.

However, given that TCCON retrieves total column estimates, and not in-situ samples as assumed by Sherwood et al. (2016), this assumption of -47‰ is a little unfair, since this is based on lower tropospheric averages, and does not take into account sink processes that occur further up into the atmosphere. For example Rigby et al. (2017) assume a -2.6‰ fractionation due to the chlorine sink in the stratosphere, and significant fractionation does occur in the troposphere with the OH sink (Röckmann et al., 2011). However, it can be argued here that the priority in calculating an accurate value of $\delta^{13}C$ from TCCON is a full

assessment of all of the systematic biases present in the retrievals, most notably the spectroscopic biases, before discussion of the true δ^{13}C value of the total column.

The results in this study have also shown the impact of water vapour is significant when considering inter-window and spectroscopic database retrievals, as identified by Figs. 11 and 9. Therefore further work is necessary to characterise the impacts on the biases exhibited in the results shown in this paper.

5   Conclusions

In this study, using the GGG2014 retrieval environment we retrieve ^{12}CH$_4$ DMFs from four TCCON sites over the course of a year in each case, with the aim of understanding the biases associated with retrieving methane in the TROPOMI spectral region as opposed to standard TCCON methane windows. Four different windows covering the spectral range of the future S5/UVNS instrument and the current S5P/TROPOMI instrument are used. Three of the windows are routinely used in TCCON products, but the TROPOMI/UVNS window in the 4190-4340 cm^{-1} range is not. We use five sources of spectroscopic parameters, the HITRAN2016, GEISA2020, SEOM-IAS and internal TCCON databases (GGG2014 and GGG2020) in order to assess the impact of spectroscopic database uncertainties.

Firstly we analysied the quality of fit of each of the windows for each of the spectroscopic databases, for each window we find the GGG2020 spectroscopic database shows the best fit metrics, except in window 1, where the SEOM-IAS database has the best quality of fit. We note that while each TCCON site shows different fit statistics for each window, the order of the spectroscopic databases in terms of quality of fit remains the same in all cases, with GGG2020 showing the best, followed by GGG2014, HITRAN2016 and GEISA2020. Window 1 shows the poorest quality fit of all of the windows, indicating room to improve the spectroscopic parameters for window 1.

Using metrics based on bias w.r.t the standard TCCON methane retrieval window (a weighted average of three windows), we found that each of the TCCON sites, the GGG2014 and GGG2020 databases exhibited normalised biases <1 in the standard TCCON windows, meaning that these biases were below the retrieval noise limit and were therefore not significant. However in window 1, both GGG2014 and GGG2020 indicated biases >1 for most of the TCCON sites, suggesting TCCON retrievals in window 1 have a significant bias to the standard TCCON window. Similarly the HITRAN and GEISA databases showed significant biases (in some cases >2) w.r.t the standard in windows 1 and 4, indicating significant disagreement between the standard TCCON retrievals and the HITRAN and GEISA databases in these windows. Only the GEISA database showed significant disagreement with the standard in windows 2 & 3, which, based on the other results shown in this paper, suggest the GEISA database as having the largest differences of all of the databases considered in this study.

The sensitivity of the retrieved ^{12}CH$_4$ DMFs to locally changing conditions such as water vapour, SZA and temperature is investigated. We find significant levels of dependence on these variations that are not necessarily mirrored across all of the TCCON sites. We conclude that some retrieval windows and spectroscopic databases are more sensitive to variable conditions than others. This sensitivity is exacerbated at TCCON locations with highly variable and challenging local conditions.

620   The δ^{13}C metric calculated in this study show significant bias w.r.t the expected total column value of -47‰. However, the use of the 4265 cm^{-1} window shows significant benefit over the 6076 cm^{-1} window, and more consistent results across spectroscopic databases. Yet, the high levels of differences between the spectroscopic databases suggest high levels of uncertainty in ^{13}CH$_4$ parameters, and further work must be done to reduce these uncertainties.

    The analysis in this study led to two key conclusions, firstly we recommend including the TROPOMI SWIR spectral region
625   (in this study, window 1) into future TCCON methane retrievals. This is based on comparable fit statistics with the original TCCON methane windows, and the significant bias w.r.t the standard TCCON retrieval product. Secondly, the different spectral windows used to generate the TCCON methane products are affected by local condition variability to varying degrees. Suggesting the weighted average normally used to generate TCCON methane products should be a unique formation depending on TCCON site and season.

630   *Code and data availability.* The GGG2014 retrieval environment is available at https://tccon-wiki.caltech.edu, and TCCON L1b spectra are available upon discussion with the relevant site PI

Appendix A: Spectral Fits
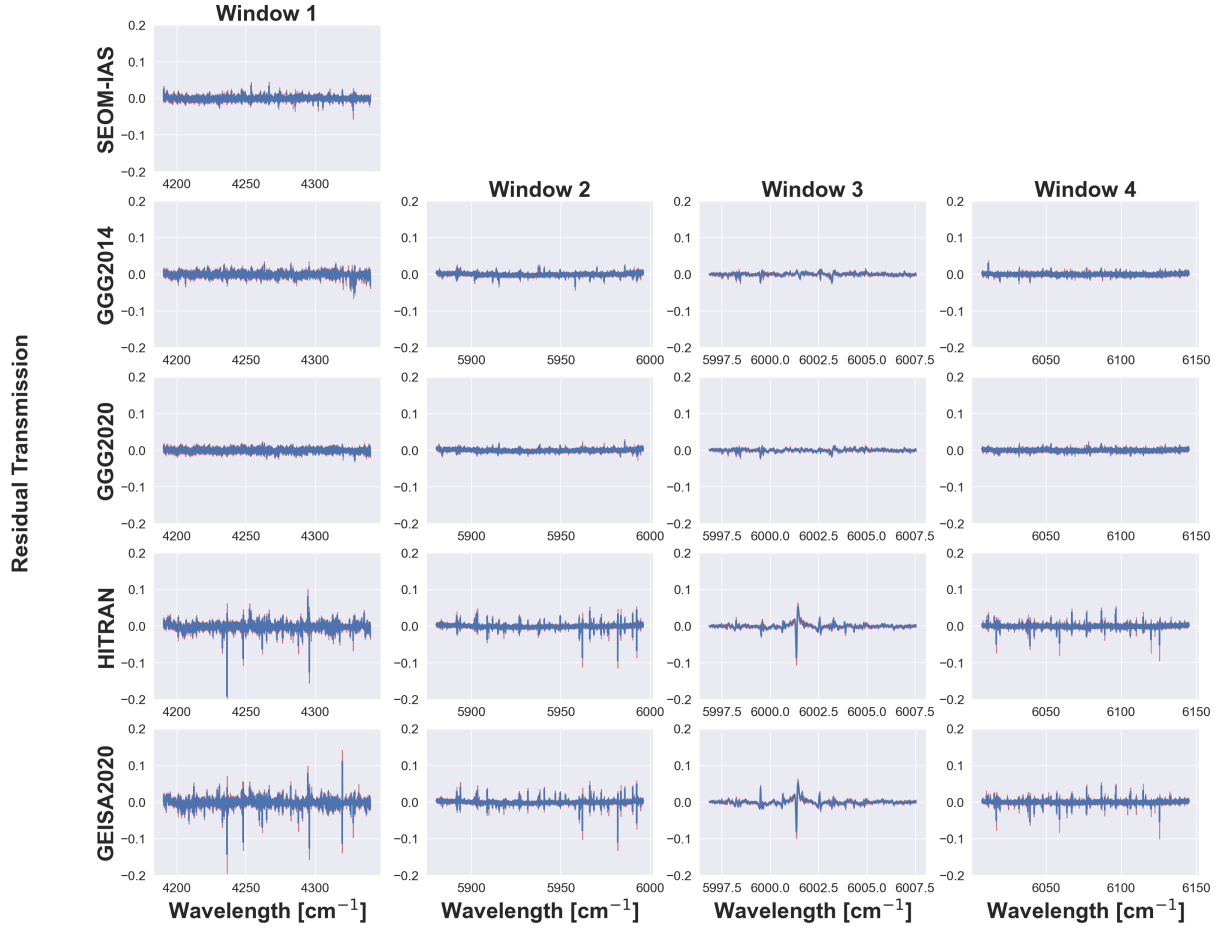
Figure A1. Example residual transmission spectra calculated from measured and fitted spectra from Darwin site in 2020.
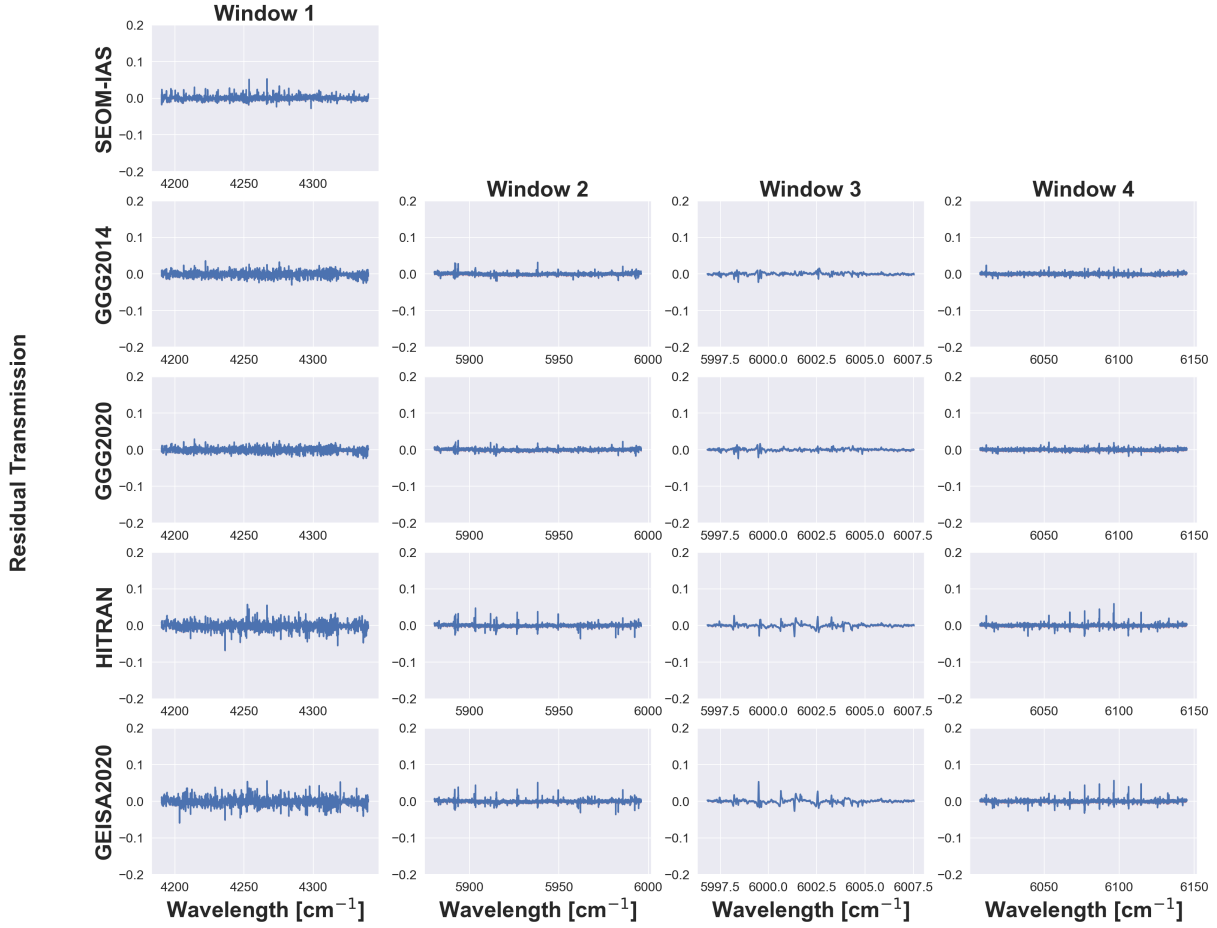
Figure A2. Example residual transmission spectra calculated from measured and fitted spectra from Tsukuba site in 2019.
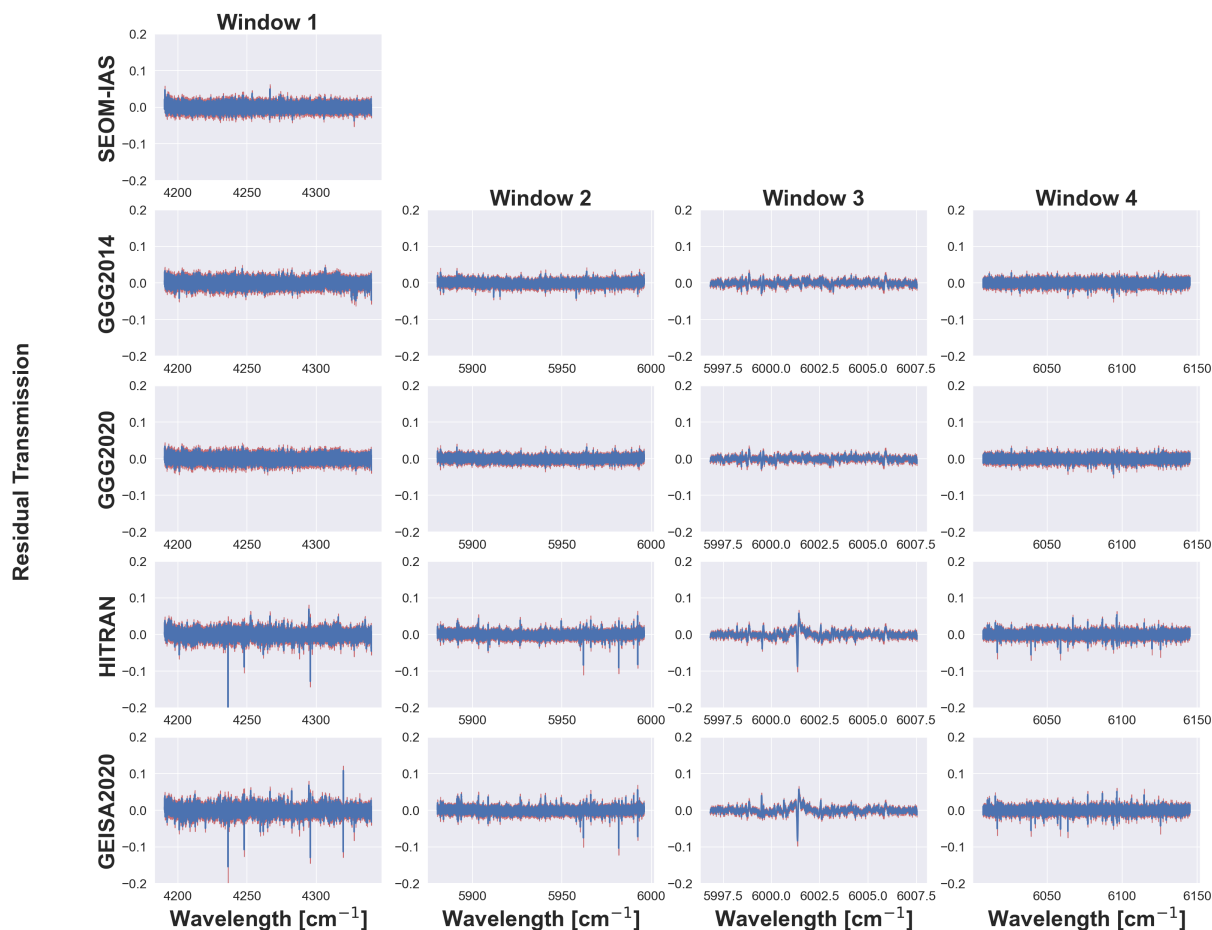
Figure A3. Example residual transmission spectra calculated from measured and fitted spectra from Ascension Island site in 2015.

Author contributions. MB provided and processed the Ny-Ålesund data, ND provided and processed the Darwin data, DGF provided and processed the Ascension Island TCCON data and IM provided and processed the Tsukuba TCCON data. EM devised and performed the study, analysed the data and wrote the paper. BV consulted on the interpretation of the results. All authors reviewed the paper.

635

Competing interests. BV is an associate editor for the joint (AMT/ACP) special issue "TROPOMI on Sentinel-5 Precursor: first year in operation". DGF is an associate editor for AMT.

Acknowledgements. This study has been performed in the framework of the postdoctoral Research Fellowship program of the European Space Agency (ESA). The GGG2014 retrieval environment was developed at the California institute of Technology (Caltech), and is available
640 at https://tccon-wiki.caltech.edu. Thanks to Geoff Toon at Caltech for providing advice on the use of GGG2014. HITRAN2016 is available at https://hitran.org/, GEISA2020 is available from http://ara.abct.lmd.polytechnique.fr/index.php?page=geisa-2. The SEOM-IAS database is available at https://www.wdc.dlr.de/seom-ias/. The TCCON line lists are described in the GGG documentation. The Ascension Island TCCON station has been supported by ESA under grant 3-14737 and by the German Bundesministerium für Wirtschaft und Energie (BMWi) under grants 50EE1711C and 50EE1711E. We thankfully acknowledge funding from the University of Bremen and the German Research
645 Foundation (DFG) – Projektnummer 268020496 – TRR 172 – (AC)3 and thank the AWIPEV station personnel in Ny-Ålesund and the Alfred-Wegener Institute Potsdam for their continuous support. The TCCON sites at Tsukuba is supported in part by the GOSAT series project. The Darwin TCCON station is funded by NASA grants NAG5- 12247 and NNG05-GD07G and supported by the Australian Research Council (ARC) grants DP1601001598, DP140101552, DP110103118, DP0879468 and LP0562346. Thanks to Anu Dudhia at Oxford University for the Fortran routine to convert the GEISA line structure into a HITRAN line structure.

650 References

(TCCON Wiki login) RunningGGG2020 < Main < TCCON Wiki, https://tccon-wiki.caltech.edu/Main/RunningGGG2020#Run_post_45Processing, 2022.

Albert, S., Bauerecker, S., Boudon, V., Brown, L., Champion, J.-P., Loëte, M., Nikitin, A., and Quack, M.: Global analysis of the high resolution infrared spectrum of methane 12CH4 in the region from 0 to 4800cm-1, Chemical Physics, 356, 131–146, https://doi.org/10.1016/j.chemphys.2008.10.019, 2009.

An, X., Caswell, A. W., and Sanders, S. T.: Quantifying the temperature sensitivity of practical spectra using a new spectroscopic quantity: Frequency-dependent lower-state energy, Journal of Quantitative Spectroscopy and Radiative Transfer, 112, 779–785, https://doi.org/10.1016/j.jqsrt.2010.10.014, 2011.

Armante, R., Scott, N., Crevoisier, C., Capelle, V., Crepeau, L., Jacquinet, N., and Chédin, A.: Evaluation of spectroscopic databases through radiative transfer simulations compared to observations. Application to the validation of GEISA 2015 with IASI and TCCON, Journal of Molecular Spectroscopy, 327, 180–192, https://doi.org/10.1016/j.jms.2016.04.004, 2016.

Bernath, P. F., McElroy, C. T., Abrams, M. C., Boone, C. D., Butler, M., Camy-Peyret, C., Carleer, M., Clerbaux, C., Coheur, P., Colin, R., DeCola, P., DeMazière, M., Drummond, J. R., Dufour, D., Evans, W. F. J., Fast, H., Fussen, D., Gilbert, K., Jennings, D. E., Llewellyn, E. J., Lowe, R. P., Mahieu, E., McConnell, J. C., McHugh, M., McLeod, S. D., Michaud, R., Midwinter, C., Nassar, R., Nichitiu, F., Nowlan, C., Rinsland, C. P., Rochon, Y. J., Rowlands, N., Semeniuk, K., Simon, P., Skelton, R., Sloan, J. J., Soucy, M., Strong, K., Tremblay, P., Turnbull, D., Walker, K. A., Walkty, I., Wardle, D. A., Wehrle, V., Zander, R., and Zou, J.: Atmospheric Chemistry Experiment (ACE): Mission overview, Geophysical Research Letters, 32, L15S01, https://doi.org/10.1029/2005GL022386, 2005.

Birk, M., Wagner, G., Loos, J., Mondelain, D., and Campargue, A.: ESA SEOM-IAS – Spectroscopic parameters database 2.3 μm region, https://doi.org/10.5281/ZENODO.1009126, 2017.

Bovensmann, H., Burrows, J. P., Buchwitz, M., Frerick, J., Noël, S., Rozanov, V. V., Chance, K. V., and Goede, A. P. H.: SCIA-MACHY: Mission Objectives and Measurement Modes, Journal of the Atmospheric Sciences, 56, 127–150, https://doi.org/10.1175/1520-0469(1999)056<0127:SMOAMM>2.0.CO;2, 1999.

Brown, L. R., Sung, K., Benner, D. C., Devi, V. M., Boudon, V., Gabard, T., Wenger, C., Campargue, A., Leshchishina, O., Kassi, S., Mondelain, D., Wang, L., Daumont, L., Régalia, L., Rey, M., Thomas, X., Tyuterev, V. G., Lyulin, O. M., Nikitin, A. V., Niederer, H. M., Albert, S., Bauerecker, S., Quack, M., O'Brien, J. J., Gordon, I. E., Rothman, L. S., Sasada, H., Coustenis, A., Smith, M. A., Carrington, T., Wang, X. G., Mantz, A. W., and Spickler, P. T.: Methane line parameters in the HITRAN2012 database, Journal of Quantitative Spectroscopy and Radiative Transfer, 130, 201–219, https://doi.org/10.1016/j.jqsrt.2013.06.020, 2013.

Buzan, E. M., Beale, C. A., Boone, C. D., and Bernath, P. F.: Global stratospheric measurements of the isotopologues of methane from the Atmospheric Chemistry Experiment Fourier transform spectrometer, Atmos. Meas. Tech, 9, 1095–1111, https://doi.org/10.5194/amt-9-1095-2016, 2016.

Checa-Garcia, R., Landgraf, J., Galli, A., Hase, F., Velazco, V. A., Tran, H., Boudon, V., Alkemade, F., and Butz, A.: Mapping spectroscopic uncertainties into prospective methane retrieval errors from Sentinel-5 and its precursor, Atmospheric Measurement Techniques, 8, 3617–3629, https://doi.org/10.5194/amt-8-3617-2015, 2015.

Crisp, D., Fisher, B. M., O 'dell, C., Frankenberg, C., Basilio, R., Bösch, H., Brown, L. R., Castano, R., Connor, B., Deutscher, N. M., Eldering, A., Griffith, D., Gunson, M., Kuze, A., Mandrake, L., Mcduffie, J., Messerschmidt, J., Miller, C. E., Morino, I., Natraj, V., Notholt, J., O 'brien, D. M., Oyafuso, F., Polonsky, I., Robinson, J., Salawitch, R., Sherlock, V., Smyth, M., Suto, H., Taylor, T. E.,

Thompson, D. R., Wennberg, P. O., Wunch, D., and Yung, Y. L.: The ACOS CO 2 retrieval algorithm – Part II: Global X CO 2 data characterization, Atmos. Meas. Tech, 5, 687–707, https://doi.org/10.5194/amt-5-687-2012, 2012.

Cygan, A., Lisak, D., Wójtewicz, S., Domysławska, J., Hodges, J. T., Trawiński, R. S., and Ciuryło, R.: High-signal-to-noise-ratio laser technique for accurate measurements of spectral line parameters, Physical Review A - Atomic, Molecular, and Optical Physics, 85, 022 508, https://doi.org/10.1103/PhysRevA.85.022508, 2012.

Delahaye, T., Armante, R., Scott, N., Jacquinet-Husson, N., Chédin, A., Crépeau, L., Crevoisier, C., Douet, V., Perrin, A., Barbe, A., Boudon, V., Campargue, A., Coudert, L., Ebert, V., Flaud, J.-M., Gamache, R., Jacquemart, D., Jolly, A., Kwabia Tchana, F., Kyuberis, A., Li, G., Lyulin, O., Manceron, L., Mikhailenko, S., Moazzen-Ahmadi, N., Müller, H., Naumenko, O., Nikitin, A., Perevalov, V., Richard, C., Starikova, E., Tashkun, S., Tyuterev, V., Vander Auwera, J., Vispoel, B., Yachmenev, A., and Yurchenko, S.: The 2020 edition of the GEISA spectroscopic database, Journal of Molecular Spectroscopy, 380, 111 510, https://doi.org/10.1016/j.jms.2021.111510, 2021.

Drummond, J. R. and Mand, G. S.: The measurements of pollution in the troposphere (MOPITT) instrument: Overall performance and calibration requirements, Journal of Atmospheric and Oceanic Technology, 13, 314–320, https://doi.org/10.1175/1520-0426(1996)013<0314:TMOPIT>2.0.CO;2, 1996.

Fisher, R. E., France, J. L., Lowry, D., Lanoisellé, M., Brownlow, R., Pyle, J. A., Cain, M., Warwick, N., Skiba, U. M., Drewer, J., Dinsmore, K. J., Leeson, S. R., Bauguitte, S. J.-B., Wellpott, A., O'Shea, S. J., Allen, G., Gallagher, M. W., Pitt, J., Percival, C. J., Bower, K., George, C., Hayman, G. D., Aalto, T., Lohila, A., Aurela, M., Laurila, T., Crill, P. M., McCalley, C. K., and Nisbet, E. G.: Measurement of the 13C isotopic signature of methane emissions from northern European wetlands, Global Biogeochemical Cycles, 31, 605–623, https://doi.org/10.1002/2016GB005504, 2017.

Galli, A., Butz, A., Scheepmaker, R. A., Hasekamp, O., Landgraf, J., Tol, P., Wunch, D., Deutscher, N. M., Toon, G. C., Wennberg, P. O., Griffith, D. W., and AbenI.: CH4, CO, and H2O spectroscopy for the Sentinel-5 Precursor mission: An assessment with the Total Carbon Column Observing Network measurements, Atmospheric Measurement Techniques, 5, 1387–1398, https://doi.org/10.5194/amt-5-1387-2012, 2012.

Gordon, I., Rothman, L., Hill, C., Kochanov, R., Tan, Y., Bernath, P., Birk, M., Boudon, V., Campargue, A., Chance, K., Drouin, B., Flaud, J.-M., Gamache, R., Hodges, J., Jacquemart, D., Perevalov, V., Perrin, A., Shine, K., Smith, M.-A., Tennyson, J., Toon, G., Tran, H., Tyuterev, V., Barbe, A., Császár, A., Devi, V., Furtenbacher, T., Harrison, J., Hartmann, J.-M., Jolly, A., Johnson, T., Karman, T., Kleiner, I., Kyuberis, A., Loos, J., Lyulin, O., Massie, S., Mikhailenko, S., Moazzen-Ahmadi, N., Müller, H., Naumenko, O., Nikitin, A., Polyansky, O., Rey, M., Rotger, M., Sharpe, S., Sung, K., Starikova, E., Tashkun, S., Auwera, J. V., Wagner, G., Wilzewski, J., Wcisło, P., Yu, S., and Zak, E.: The HITRAN2016 Molecular Spectroscopic Database, Journal of Quantitative Spectroscopy and Radiative Transfer, https://doi.org/10.1016/j.jqsrt.2017.06.038, 2017.

Hu, H., Hasekamp, O., Butz, A., Galli, A., Landgraf, J., Aan De Brugh, J., Borsdorff, T., Scheepmaker, R., and Aben, I.: The operational methane retrieval algorithm for TROPOMI, Atmos. Meas. Tech, 9, 5423–5440, https://doi.org/10.5194/amt-9-5423-2016, 2016.

Ingmann, P., Veihelmann, B., Langen, J., Lamarre, D., Stark, H., and Courrèges-Lacoste, G. B.: Requirements for the GMES Atmosphere Service and ESA's implementation concept: Sentinels-4/-5 and -5p, Remote Sensing of Environment, 120, 58–69, https://doi.org/10.1016/J.RSE.2012.01.023, 2012.

IPCC: Fifth Assessment Report - Impacts, Adaptation and Vulnerability, http://www.ipcc.ch/report/ar5/wg2/, 2014.

Jacquinet-Husson, N., Armante, R., Scott, N. A., Chédin, A., Crépeau, L., Boutammine, C., Bouhdaoui, A., Crevoisier, C., Capelle, V., Boonne, C., Poulet-Crovisier, N., Barbe, A., Chris Benner, D., Boudon, V., Brown, L. R., Buldyreva, J., Campargue, A., Coudert, L. H., Devi, V. M., Down, M. J., Drouin, B. J., Fayt, A., Fittschen, C., Flaud, J. M., Gamache, R. R., Harrison, J. J., Hill, C., Hodnebrog, Hu,

725   S. M., Jacquemart, D., Jolly, A., Jiménez, E., Lavrentieva, N. N., Liu, A. W., Lodi, L., Lyulin, O. M., Massie, S. T., Mikhailenko, S., Müller, H. S., Naumenko, O. V., Nikitin, A., Nielsen, C. J., Orphal, J., Perevalov, V. I., Perrin, A., Polovtseva, E., Predoi-Cross, A., Rotger, M., Ruth, A. A., Yu, S. S., Sung, K., Tashkun, S. A., Tennyson, J., Tyuterev, V. G., Vander Auwera, J., Voronin, B. A., and Makie, A.: The 2015 edition of the GEISA spectroscopic database, Journal of Molecular Spectroscopy, 327, 31–72, https://doi.org/10.1016/j.jms.2016.06.007, 2016.

730   Kirschke, S., Bousquet, P., Ciais, P., Saunois, M., Canadell, J. G., Dlugokencky, E. J., Bergamaschi, P., Bergmann, D., Blake, D. R., Bruhwiler, L., Cameron-Smith, P., Castaldi, S., Chevallier, F., Feng, L., Fraser, A., Heimann, M., Hodson, E. L., Houweling, S., Josse, B., Fraser, P. J., Krummel, P. B., Lamarque, J. F., Langenfelds, R. L., Le Quéré, C., Naik, V., O'doherty, S., Palmer, P. I., Pison, I., Plummer, D., Poulter, B., Prinn, R. G., Rigby, M., Ringeval, B., Santini, M., Schmidt, M., Shindell, D. T., Simpson, I. J., Spahni, R., Steele, L. P., Strode, S. A., Sudo, K., Szopa, S., Van Der Werf, G. R., Voulgarakis, A., Van Weele, M., Weiss, R. F., Williams, J. E., and Zeng, G.: Three decades of
735   global methane sources and sinks, https://doi.org/10.1038/ngeo1955, 2013.

Laughner, J., Andrews, A., Roche, S., Kiel, M., and Toon, G.: ginput v1.0.10: GGG2020 prior profile software (Version 1.0.10), https://doi.org/10.22002/D1.1944, 2021.

Lorente, A., Borsdorff, T., Butz, A., Hasekamp, O., Aan De Brugh, J., Schneider, A., Wu, L., Hase, F., Kivi, R., Wunch, D., Pollard, D. F., Shiomi, K., Deutscher, N. M., Velazco, V. A., Roehl, C. M., Wennberg, P. O., Warneke, T., and Landgraf, J.: Methane retrieved from
740   TROPOMI: Improvement of the data product and validation of the first 2 years of measurements, Atmospheric Measurement Techniques, 14, 665–684, https://doi.org/10.5194/amt-14-665-2021, 2021.

Malina, E., Yoshida, Y., Matsunaga, T., and Muller, J. P.: Information content analysis: The potential for methane isotopologue retrieval from GOSAT-2, Atmospheric Measurement Techniques, 11, 1159–1179, https://doi.org/10.5194/amt-11-1159-2018, 2018.

Malina, E., Hu, H., Landgraf, J., and Veihelmann, B.: A study of synthetic 13 CH 4 retrievals from TROPOMI and Sentinel-5/UVNS, Atmos.
745   Meas. Tech, 12, 6273–6301, https://doi.org/10.5194/amt-12-6273-2019, 2019.

Mendonca, J., Strong, K., Sung, K., Devi, V. M., Toon, G. C., Wunch, D., and Franklin, J. E.: Using high-resolution laboratory and ground-based solar spectra to assess CH4 absorption coefficient calculations, Journal of Quantitative Spectroscopy and Radiative Transfer, 190, 48–59, https://doi.org/10.1016/j.jqsrt.2016.12.013, 2017.

Ngo, N. H., Lisak, D., Tran, H., and Hartmann, J. M.: An isolated line-shape model to go beyond the Voigt profile in spec-
750   troscopic databases and radiative transfer codes, Journal of Quantitative Spectroscopy and Radiative Transfer, 129, 89–100, https://doi.org/10.1016/j.jqsrt.2013.05.034, 2013.

Nikitin, A., Lyulin, O., Mikhailenko, S., Perevalov, V., Filippov, N., Grigoriev, I., Morino, I., Yoshida, Y., and Matsunaga, T.: GOSAT-2014 methane spectral line list, Journal of Quantitative Spectroscopy and Radiative Transfer, 154, 63–71, https://doi.org/10.1016/J.JQSRT.2014.12.003, 2015.

755   Nikitin, A., Chizhmakova, I., Rey, M., Tashkun, S., Kassi, S., Mondelain, D., Campargue, A., and Tyuterev, V.: Analysis of the absorption spectrum of 12CH4 in the region 5855–6250 cm-1 of the $2\nu 3$ band, Journal of Quantitative Spectroscopy and Radiative Transfer, 203, 341–348, https://doi.org/10.1016/J.JQSRT.2017.05.014, 2017.

Nisbet, E. G., Dlugokencky, E. J., Manning, M. R., Lowry, D., Fisher, R. E., France, J. L., Michel, S. E., Miller, J. B., White, J. W. C., Vaughn, B., Bousquet, P., Pyle, J. A., Warwick, N. J., Cain, M., Brownlow, R., Zazzeri, G., Lanoisellé, M., Manning, A. C., Gloor, E.,
760   Worthy, D. E. J., Brunke, E.-G., Labuschagne, C., Wolff, E. W., and Ganesan, A. L.: Rising atmospheric methane: 2007-2014 growth and isotopic shift, Global Biogeochemical Cycles, 30, 1356–1370, https://doi.org/10.1002/2016GB005406, 2016.

Rella, C. W., Hoffnagle, J., He, Y., and Tajima, S.: Local-and regional-scale measurements of CH 4 , δ 13 CH 4 , and C 2 H 6 in the Uintah Basin using a mobile stable isotope analyzer, Atmos. Meas. Tech, 8, 4539–4559, https://doi.org/10.5194/amt-8-4539-2015, 2015.

Rigby, M., Montzka, S. A., Prinn, R. G., White, J. W. C., Young, D., O'Doherty, S., Lunt, M. F., Ganesan, A. L., Manning, A. J., Simmonds, P. G., Salameh, P. K., Harth, C. M., Mühle, J., Weiss, R. F., Fraser, P. J., Steele, L. P., Krummel, P. B., McCulloch, A., and Park, S.: Role of atmospheric oxidation in recent methane growth., Proceedings of the National Academy of Sciences of the United States of America, 114, 5373–5377, https://doi.org/10.1073/pnas.1616426114, 2017.

Röckmann, T., Brass, M., Borchers, R., and Engel, A.: The isotopic composition of methane in the stratosphere: High-altitude balloon sample measurements, Atmospheric Chemistry and Physics, 11, 13 287–13 304, https://doi.org/10.5194/acp-11-13287-2011, 2011.

Saunois, M., Stavert, A. R., Poulter, B., Bousquet, P., Canadell, J. G., Jackson, R. B., Raymond, P. A., Dlugokencky, E. J., Houweling, S., Patra, P. K., Ciais, P., Arora, V. K., Bastviken, D., Bergamaschi, P., Blake, D. R., Brailsford, G., Bruhwiler, L., Carlson, K. M., Carrol, M., Castaldi, S., Chandra, N., Crevoisier, C., Crill, P. M., Covey, K., Curry, C. L., Etiope, G., Frankenberg, C., Gedney, N., Hegglin, M. I., Höglund-Isakson, L., Hugelius, G., Ishizawa, M., Ito, A., Janssens-Maenhout, G., Jensen, K. M., Joos, F., Kleinen, T., Krummel, P. B., Langenfelds, R. L., Laruelle, G. G., Liu, L., Machida, T., Maksyutov, S., McDonald, K. C., McNorton, J., Miller, P. A., Melton, J. R., Morino, I., Müller, J., Murgia-Flores, F., Naik, V., Niwa, Y., Noce, S., O'Doherty, S., Parker, R. J., Peng, C., Peng, S., Peters, G. P., Prigent, C., Prinn, R., Ramonet, M., Regnier, P., Riley, W. J., Rosentreter, J. A., Segers, A., Simpson, I. J., Shi, H., Smith, S. J., Steele, P. L., Thornton, B. F., Tian, H., Tohjima, Y., Tubiello, F. N., Tsuruta, A., Viovy, N., Voulgarakis, A., Weber, T. S., van Weele, M., van der Werf, G. R., Weiss, R. F., Worthy, D., Wunch, D., Yin, Y., Yoshida, Y., Zhang, W., Zhang, Z., Zhao, Y., Zheng, B., Zhu, Q., Zhu, Q., and Zhuang, Q.: The Global Methane Budget 2000-2017, Earth System Science Data Discussions, pp. 1–138, https://doi.org/10.5194/essd-2019-128, 2019.

Scheepmaker, R. A., Aan De Brugh, J., Hu, H., Borsdorff, T., Frankenberg, C., Risi, C., Hasekamp, O., Aben, I., and Landgraf, J.: HDO and H2O total column retrievals from TROPOMI shortwave infrared measurements, Atmospheric Measurement Techniques, 9, 3921–3937, https://doi.org/10.5194/amt-9-3921-2016, 2016.

Schneising, O., Buchwitz, M., Reuter, M., Bovensmann, H., Burrows, J. P., Borsdorff, T., Deutscher, N. M., Feist, D. G., Griffith, D. W. T., Hase, F., Hermans, C., Iraci, L. T., Kivi, R., Landgraf, J., Morino, I., Notholt, J., Petri, C., Pollard, D. F., Roche, S., Shiomi, K., Strong, K., Sussmann, R., Velazco, V. A., Warneke, T., and Wunch, D.: A scientific algorithm to simultaneously retrieve carbon monoxide and methane from TROPOMI onboard Sentinel-5 Precursor, Atmospheric Measurement Techniques Discussions, pp. 1–44, https://doi.org/10.5194/amt-2019-243, 2019.

Sherwood, O., Schwietzke, S., Arling, V., and Etiope, G.: Global Inventory of Fossil and Non-fossil Methane δ13C Source Signature Measurements for Improved Atmospheric Modeling, https://doi.org/10.15138/G37P4D, 2016.

TCCON: Using the cc option in GGG2014 - Tccon-wiki, https://tccon-wiki.caltech.edu/index.php?title=Software/GGG/Download/ GGG{_}2014{_}Release{_}Notes/Using{_}the{_}cc{_}option{_}in{_}GGG2014{&}highlight=continuum+curvature, 2020.

Toon, G. C.: Atmospheric Line List for the 2014 TCCON Data Release, https://doi.org/10.14291/tccon.ggg2014.atm.R0/1221656, 2015.

Tran, H., Ngo, N., and Hartmann, J.-M.: Efficient computation of some speed-dependent isolated line profiles, Journal of Quantitative Spectroscopy and Radiative Transfer, 129, 199–203, https://doi.org/10.1016/J.JQSRT.2013.06.015, 2013.

Veefkind, J. P., Aben, I., McMullan, K., Förster, H., de Vries, J., Otter, G., Claas, J., Eskes, H. J., de Haan, J. F., Kleipool, Q., van Weele, M., Hasekamp, O., Hoogeveen, R., Landgraf, J., Snel, R., Tol, P., Ingmann, P., Voors, R., Kruizinga, B., Vink, R., Visser, H., and Levelt, P. F.: TROPOMI on the ESA Sentinel-5 Precursor: A GMES mission for global observations of the atmospheric composition for climate, air quality and ozone layer applications, Remote Sensing of Environment, 120, 70–83, https://doi.org/10.1016/j.rse.2011.09.027, 2012.

800 Weidmann, D., Hoffmann, A., Macleod, N., Middleton, K., Kurtz, J., Barraclough, S., and Griffin, D.: The Methane Isotopologues by Solar Occultation (MISO) Nanosatellite Mission: Spectral Channel Optimization and Early Performance Analysis, Remote Sensing, 9, 1073, https://doi.org/10.3390/rs9101073, 2017.

Wunch, D., Toon, G. C., Wennberg, P. O., Wofsy, S. C., Stephens, B. B., Fischer, M. L., Uchino, O., Abshire, J. B., Bernath, P., Biraud, S. C., Blavier, J.-F. L., Boone, C., Bowman, K. P., Browell, E. V., Campos, T., Connor, B. J., Daube, B. C., Deutscher, N. M., Diao, M., Elkins,
805 J. W., Gerbig, C., Gottlieb, E., Griffith, D. W. T., and Hurst, D. F.: Calibration of the Total Carbon Column Observing Network using aircraft profile data, Atmos. Meas. Tech, 3, 1351–1362, https://doi.org/10.5194/amt-3-1351-2010, 2010.

Wunch, D., Toon, G. C., Blavier, J.-F. L., Washenfelder, R. A., Notholt, J., Connor, B. J., Griffith, D. W. T., Sherlock, V., and Wennberg, P. O.: The Total Carbon Column Observing Network, Phil. Trans. R. Soc. A, 369, 2087–2112, https://doi.org/10.1098/rsta.2010.0240, 2011.

Wunch, D., Toon, G., Sherlock, V., Deutscher, N., Liu, C., Feist, D., and Wennberg, P.: The Total Carbon Column Observing Network's
810 GGG2014 Data Version, Tech. rep., https://doi.org/10.14291/tccon.ggg2014.documentation.R0/1221662, 2015.

Yoshida, Y., Ota, Y., Eguchi, N., Kikuchi, N., Nobuta, K., Tran, H., Morino, I., and Yokota, T.: Retrieval algorithm for CO 2 and CH 4 column abundances from short-wavelength infrared spectral observations by the Greenhouse gases observing satellite, Atmos. Meas. Tech, 4, 717–734, https://doi.org/10.5194/amt-4-717-2011, 2011.

Yoshida, Y., Kikuchi, N., Morino, I., Uchino, O., Oshchepkov, S., Bril, A., Saeki, T., Schutgens, N., Toon, G. C., Wunch, D., Roehl, C. M.,
815 Wennberg, P. O., Griffith, D. W. T., Deutscher, N. M., Warneke, T., Notholt, J., Robinson, J., Sherlock, V., Connor, B., Rettinger, M., Sussmann, R., Ahonen, P., Heikkinen, P., Kyrö, E., Mendonca, J., Strong, K., Hase, F., Dohe, S., and Yokota, T.: Improvement of the retrieval algorithm for GOSAT SWIR XCO2 and XCH4 and their validation using TCCON data, Atmospheric Measurement Techniques, 6, 1533–1547, https://doi.org/10.5194/amt-6-1533-2013, 2013.

Zhou, M., Langerock, B., Sha, M. K., Kumps, N., Hermans, C., Petri, C., Warneke, T., Chen, H., Metzger, J. M., Kivi, R., Heikkinen, P.,
820 Ramonet, M., and De Mazière, M.: Retrieval of atmospheric CH4 vertical information from ground-based FTS near-infrared spectra, Atmospheric Measurement Techniques, 12, 6125–6141, https://doi.org/10.5194/amt-12-6125-2019, 2019.